



POLITECNICO DI TORINO

Faculty of Engineering

Master Degree in Communications and Computer
Networks Engineering

Master Thesis

**Analysis and Testing of an X-Band
Deep-Space Radio System for
Nanosatellites**

Mentor

Prof. Roberto Garelo

Candidate

Pasquale Tricarico

October 2019

To my family and to those who have been there for me

Alla mia famiglia e a chi mi è stato vicino

Abstract

This thesis provides a description of analysis, performance and tests of an X-Band radio system for nanosatellites. The thesis work has been carried out in collaboration with the Italian aerospace company Argotec in Turin supported by Politecnico di Torino. The scope of the thesis is the ArgoMoon mission which will start on June 2020. ArgoMoon is a nanosatellite developed by Argotec in coordination with the Italian Space Agency (ASI). After an introduction to the mission, follows a description of the entire communication system including NASA Deep Space Network (DSN), spacecraft telecommunication subsystem and a set of involved Consultative Committee for Space Data System (CCSDS) Standards. The main guideline has been the Telecommunication Link Design Handbook written by NASA JPL, which gives essential information for the subsequent communication link analysis, supported by CCSDS Standards and further publications. A set of communication link performance analysis methods and results are provided for two relevant communication scenarios. Concurrently, compatibility tests have been carried out to assess ArgoMoon satellite to DSN interface performance and compatibility. The document ends with the description of a system which will act as Ground Support Equipment during the satellite validation tests.

Acknowledgements

I would like to thank prof. Roberto Garello for his availability during this thesis work and for the pleasure and involvement felt in attending each of his lessons.

I would like to thank all of those who have always supported me in this long journey, my mother Teresa, my father Enzo and my brothers Fabio and Christian. A special thanks to the latter for making me find the strength to undertake my university career.

I also wish to thank my lifelong friends, when in addition to the study they were taking care of having some quality time together.

I want to show my appreciation to Argotec working group and in particular to the avionics unit, for the time spent together, for the useful comparisons and learning.

I conclude with a sincere thanks to a person who most has been close by me, supporting me and (putting up with me) in study and in the life, isn't it Cí?

Desidero ringraziare il prof. Roberto Garelo per la sua disponibilità durante questo lavoro di tesi e per il piacere e il coinvolgimento provati all'ascolto di ogni sua lezione.

Ringrazio tutti coloro che da sempre mi hanno supportato in questo lungo percorso, mia madre Teresa, mio padre Enzo e i miei fratelli Fabio e Christian. Un grazie particolare a quest'ultimo per avermi fatto trovare la forza per intraprendere la mia carriera universitaria.

Ringrazio i miei amici di una vita, quando oltre allo studio ci pensavano loro a farmi passare dei bei momenti.

Ringrazio il gruppo di lavoro in Argotec e in particolare il gruppo avionica, per il tempo trascorso insieme, per gli utili confronti e gli apprendimenti.

Concludo con un ringraziamento sincero a chi più di tutti mi è stato accanto supportandomi e (sopportandomi) nello studio e nella vita, no Cí?

Contents

Acknowledgements	iv
Contents	vi
List of Figures	ix
List of Tables	xi
Acronyms	xii
Chapter 1 Introduction	1
1.1 Motivation	1
1.2 Objectives	2
1.3 Thesis Outline	2
Chapter 2 Artemis 1 - Mission Overview	4
2.1 Mission Description	5
2.2 The CubeSat Concept	7
Chapter 3 Communication System	9
3.1 NASA Deep-Space Network	9
3.1.1 Ground Station Specifications.....	10
3.1.2 Frequency Bands Allocation.....	10
3.1.3 DSN Services	12
3.2 ArgoMoon Telecom Subsystem	13
3.3 Telemetry and Telecommand	14
3.3.1 Telemetry Overview.....	14
3.3.2 Telemetry: Physical Layer	15
3.3.3 Telemetry: Systems Loss Models.....	15
3.3.4 Telemetry: Coding Layer	16
3.3.5 Telecommand Overview	19

3.3.6	Telecommand: BCH Encoding	20
3.3.7	Telecommand: Communication Link Transmission Unit.....	21
3.3.8	Telecommand: Physical Layer and Operation Procedures	21
3.4	Ranging	23
3.4.1	Sequential Ranging	24
3.4.2	PN Ranging.....	24
Chapter 4	<i>Link Budget Analysis.....</i>	25
4.1	Free Space Path and Atmospheric Losses	25
4.2	Antenna Gains.....	25
4.2.1	ArgoMoon Antenna Gain	26
4.2.2	DSN Antenna Gain	28
4.3	System Noise Temperatures.....	29
4.3.1	Noise Temperature for ArgoMoon Receiver.....	30
4.3.2	Noise Temperature for DSN Stations.....	31
Chapter 5	<i>Mission Analysis and System Performances</i>	36
5.1	ArgoMoon Mission Phase 1	36
5.2	ArgoMoon Mission Phase 2	41
5.3	Power Allocation.....	44
5.4	Telemetry Performance.....	44
5.5	Command Performance.....	46
5.6	Sequential Ranging Performance.....	47
5.7	Pseudo-Noise Ranging Performance.....	47
Chapter 6	<i>Compatibility and Functional Tests</i>	49
6.1	DSN Compatibility Tests	49
6.1.1	RF Link Calibration	50
6.1.2	Uplink Receiver Threshold and AGC Calibration.....	51
6.1.3	Uplink Receiver Acquisition and Tracking.....	51
6.1.4	Uplink Receiver Tracking Range.....	52

6.1.5	Command and Telemetry Performance.....	52
6.1.6	Range Delay and Polarity.....	53
6.2	Ground Support Equipment for Functional Tests	53
Chapter 7	<i>Final Remarks</i>.....	54
7.1	Conclusion	54
7.2	Future Works	56
References	57

List of Figures

Figure 2-1 Block 1 Initial SLS Configuration [2].....	4
Figure 2-2 Block 1 Initial SLS Configuration [2].....	5
Figure 2-3 ICPS Operations after TLI [1]	6
Figure 2-4 ArgoMoon Mission Phases	7
Figure 2-5 ArgoMoon Representation.....	8
Figure 3-1 NASA DSN Antenna Location [3]	9
Figure 3-2 ArgoMoon Telecom Subsystem Block Diagram.....	13
Figure 3-3 Layered Telemetry Service Model [7]	15
Figure 3-4 Performance Comparison of Selected Convolutional, Reed-Solomon, Concatenated and Turbo Code [7]	17
Figure 3-5 Bit Rate and Symbol Rate Terminology [10].....	18
Figure 3-6 Telemetry Data Structure for Turbo Code [7]	18
Figure 3-7 Procedures at Sending End (Left) and Receiving End (Right) [21]	19
Figure 3-8 Format of a BCH Codeblock [21]	20
Figure 3-9 Format of a CLTU [21]	21
Figure 3-10 Frame Rejection Probability in Single Error Correction Mode for the Last or Only Frame in a CLTU (PLOP-2) [21]	22
Figure 4-1 Typical Antenna Radiation Pattern.....	26
Figure 4-2 Radiation Pattern for TX Antenna (Central Frequency 8.475 GHz)	27
Figure 4-3 Radiation Pattern for RX Antenna (Central Frequency 7.213 GHz)	27
Figure 4-4 Operative Temperature Illustration	29
Figure 4-5 Canberra DSS-34 (HEMT Diplexed) System Operative Temperature as Function of Elevation Angle (February).....	34
Figure 4-6 Goldstone DSS-24 (Maser Diplexed) System Operative Temperature as Function of Elevation Angle (February).....	34

Figure 5-1 Phase 1 - First Acquisition Communication Scenario - ArgoMoon Altitude 31210 km	41
Figure 5-2 Phase 2 – After Last Lunar Fly-by Communication Scenario - ArgoMoon Altitude 409768 km	43
Figure 6-1 Transponder-to-CTT Connection	50
Figure 6-2 Transponder-to-CTT connection. Variable Attenuations	50
Figure 6-3 Frequency Sweep Profile for Carrier Acquisition and Tracking	51
Figure 6-4 Frequency Sweep Profile for Carrier Tracking Range	52

List of Tables

Table 3-1 Frequency Bands (in MHz) Available at DSN Stations	11
Table 3-2 Transponding Ratios	12
Table 4-1 Hot Body Brightness Temperature at X-Band.....	30
Table 4-2 Antenna Parameters for <i>TAMW</i> Computation	33
Table 5-1 Phase 1 - Goldstone Ground Station Fundamental Estimated Parameters	37
Table 5-2 Phase 1 - Canberra Ground Station Fundamental Estimated Parameters	38
Table 5-3 Phase 1 - Madrid Ground Station Fundamental Estimated Parameters	38
Table 5-4 Phase 1 - Ground Station and Link Parameters	39
Table 5-5 Phase 1 - Receivers Parameters.....	40
Table 5-6 Phase 2 - Canberra Ground Station Fundamental Estimated Parameters	42
Table 5-7 Phase 2 - Ground Station and Link Parameters	42
Table 5-8 Phase 2 - Receivers Parameters.....	43
Table 5-9 Phase 1 - Downlink Power Allocation	44
Table 5-10 Phase 1 - Telemetry Performances and Link Margin @ 256kbps	45
Table 5-11 Phase 2 - Downlink Power Allocation	46
Table 5-12 Phase 2 - Telemetry Performances and Link Margin @ 256kbps	46
Table 5-13 Phase 1 - Command Performances and Link Margin @ 4kbps	47
Table 5-14 Phase 2 - Command Performances and Link Margin @ 4kbps	47

Acronyms

AGC	Automatic Gain Control
ASM	Attached Sync Marker
BCH	Bose-Chaudhuri-Hoquenghem
BER	Bit Error Rate
BLF	Best Lock Frequency
BWG	Beam Waveguide
CLTU	Communication Link Transmission Unit
CMB	Cosmic Microwave Background
CMF	Cosmic Microwave Foreground
CTT	Compatibility Test Trailer
CW	Continuous Wave
DOR	Differential One-Way Ranging
DS	Deep Space
DSN	Deep Space Network
DTF	Development Test Facility
FER	Frame Error Rate
FSPL	Free-Space Path Loss
GSE	Ground Support Equipment
HEF	High Efficiency
ITU	International Telecommunication Union
LCP	Left Circular Polarization
LNA	Low Noise Amplifier
MCC	Mission Control Centre
NA	Not Available
NE	Near Earth
PLL	Phase-Locked Loop
PLOP	Physical Layer and Operation Procedures
PN	Pseudo-Noise
RCP	Right Circular Polarization
RF	Radio Frequency
RFS	Radio Frequency Subsystem
RU	Range Unit
SNR	Signal-to-Noise Ratio
SSPA	Solid-State Power Amplifier
TC	Telecommand
TLI	Trans-Lunar Injection
TM	Telemetry
USRP	Universal Software Radio Peripheral

Chapter 1

Introduction

1.1 Motivation

Space exploration has always been one of the things that fascinated man. The constant search for knowledge will never end in a boundless and unlimited space. Important government bodies or private entities have been working to achieve this kind of goals since years.

Knowing that you can rely on reliable communication is the sought certainty by a space mission. In the absolute empty space there is no possibility of physical intervention if something goes wrong. One is the medium capable of carrying information through astronomic distances: the electromagnetic wave. Very often not perceptible by any of the human senses, except in the optical domain. NASA Deep Space Network provides services on a solid and now consolidated telecommunication infrastructure, for communications reaching the limits of the solar system.

CubeSats' world, or nanosatellites, is constantly expanding. They are compact satellites even in terms of cost. Very often they are carried into space as secondary payloads on spacecrafts launchers of much greater dimensions. Many of them have been designed by university students and sent to Low Earth Orbit (LEO), while others have even left the LEO. This is the case of MarCo, developed by NASA, a couple of CubeSat that first participated to a deep space mission by reaching the orbit of Mars.

ArgoMoon spacecraft is a CubeSat entirely built by the Italian aerospace company Argotec in coordination with the Italian Space Agency (ASI). ArgoMoon will follow a high elliptical orbit, orbiting beyond the Moon until it will pass to a heliocentric

orbit, orbiting around the Sun. The topic of this thesis is the telecommunication system of which ArgoMoon is part involving NASA DSN, providing analysis of its fundamental aspects and indispensable results for the mission.

1.2 Objectives

The goal of this master's thesis is to explore, analyse and test an X-Band Deep-Space radio system for nanosatellites. One of the largest communication infrastructures on Earth will be involved, NASA DSN, whose compatibility with on-board avionics will be tested at the DSN's facility DTF-21, in Monrovia (CA).

The main objectives for this thesis project are described in the following list.

- Define standards, recommendations and regulations study for a satellite communication
- Explore and study all the parts the communication system is composed of
- Analyse the satellite link including:
 - Signal attenuation, atmospheric effects and signal propagation delay
 - Receivers and noise contribution
- Analyze and evaluate results and performances
- Put up mission control tables to allow optimal communication windows allocation during the mission
- Perform compatibility and functional test of the flight hardware

1.3 Thesis Outline

This paragraph describes how this thesis is organized giving a small description of the content of each chapter.

Chapter 2 provides some details of the new Space Launch System that will bring ArgoMoon satellite into space. Follows a description of ArgoMoon mission and its main phases. At the end some general information about the CubeSat's world and in particular ArgoMoon satellite.

Chapter 3 gives a description of the entire communication systems involved in the ArgoMoon mission. In the first part a description of NASA Deep Space Network, then a description of ArgoMoon telecom subsystem. Particular focus is given to telecommand, telemetry and ranging signals.

Chapter 4 describes all the techniques and strategies adopted in the link budget analysis for ArgoMoon mission. Signal attenuation and atmospheric losses are analysed in general. Receiver noise temperatures are differentiated for DSN and ArgoMoon receiver.

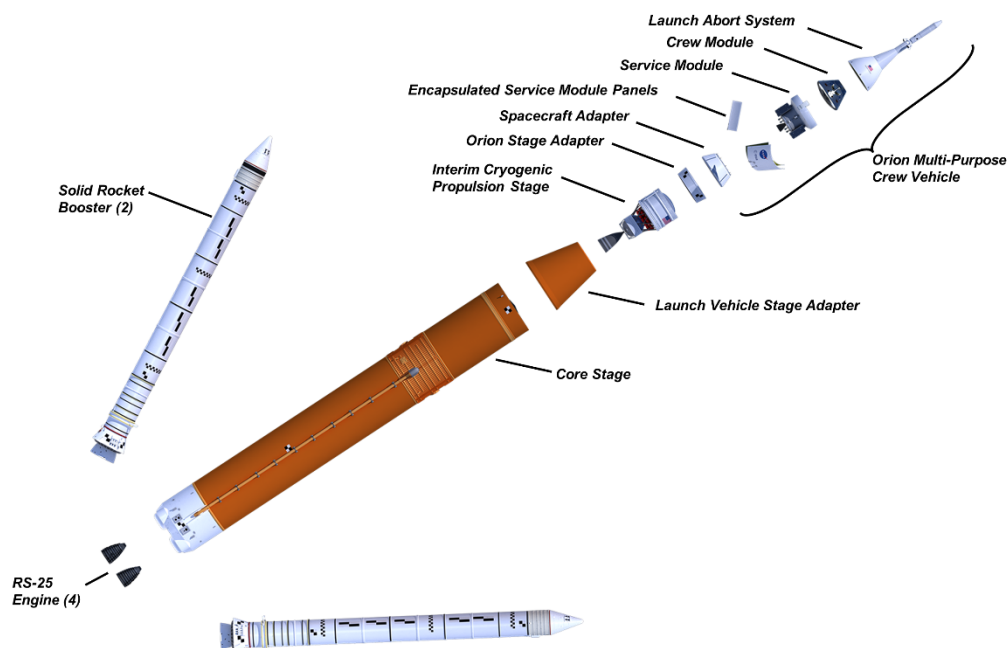
Chapter 5 provides information extracted from ArgoMoon mission analysis, including ground station parameters and system performances evaluation in two communication scenarios.

Chapter 6 reports test performed directly onto the flight hardware in order to asses DSN compatibility. Then, a description of a Ground Support Equipment for further functional tests to be performed in Argotec (Turin) after the satellite assembly.

Chapter 2

Mission Overview

ArgoMoon is one of the thirteen nanosatellites that will be launched during the NASA Artemis 1, previously known as Exploration Mission 1 (EM1), as secondary payload of the Space Launch System (SLS). The main purpose of Artemis 1 is to test the new launch system that will bring the human being further the Low Earth Orbit (LEO) reaching the Moon, asteroids and possibly Mars.



2

Figure 2-1 Block 1 Initial SLS Configuration [2]

SLS (Figure 2-1) is an advanced launch vehicle that, during Artemis 1, is able to send an unmanned spacecraft, called Orion, to a stable orbit beyond the Moon. In the future, Orion will bring a crew of four astronauts and cargo to the Moon or

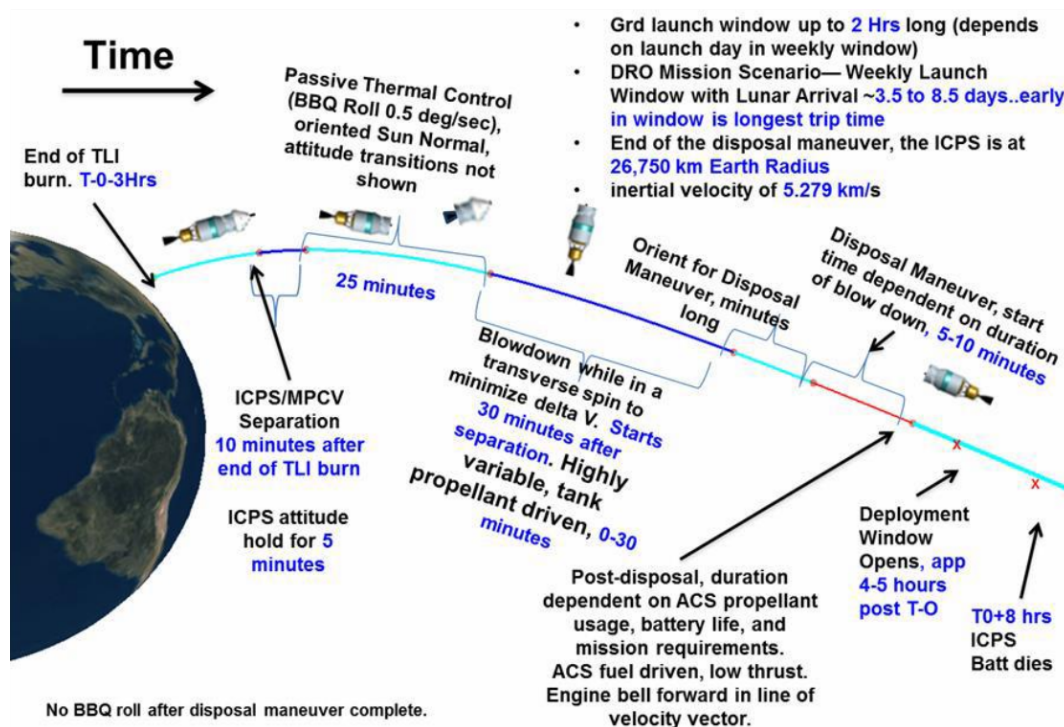


Figure 2-3 ICPS Operations after TLI [1]

Here the importance of ArgoMoon, it will take high-definition pictures of ICPS providing to NASA scientific information that can testify the correct execution of the operations of the launcher.

ArgoMoon mission has been divided into two main phases, called Phase 1 and Phase 2.

Phase 1 starts with the deployment and lasts for the first 10 hours of mission. This phase can be divided into two sub-phases:

- ICPS observation
- Manoeuvring for catching and taking advantage of the first Moon flyby

The main objective of the Phase 1 is to take photographs of ICPS and pictures that confirm the other nanosatellites have been successfully released. During this phase the propulsion system will be heated up, ready to perform some relative dynamic manoeuvres to maintain ArgoMoon close to ICPS

During the Phase 2 the satellite will keep orbiting the Earth for 165 days, then the satellite will perform a final disposal flyby to escape the Earth gravity field,

continuing along a heliocentric trajectory. Figure 2-4 shows the mission phases up to the final disposal orbit.

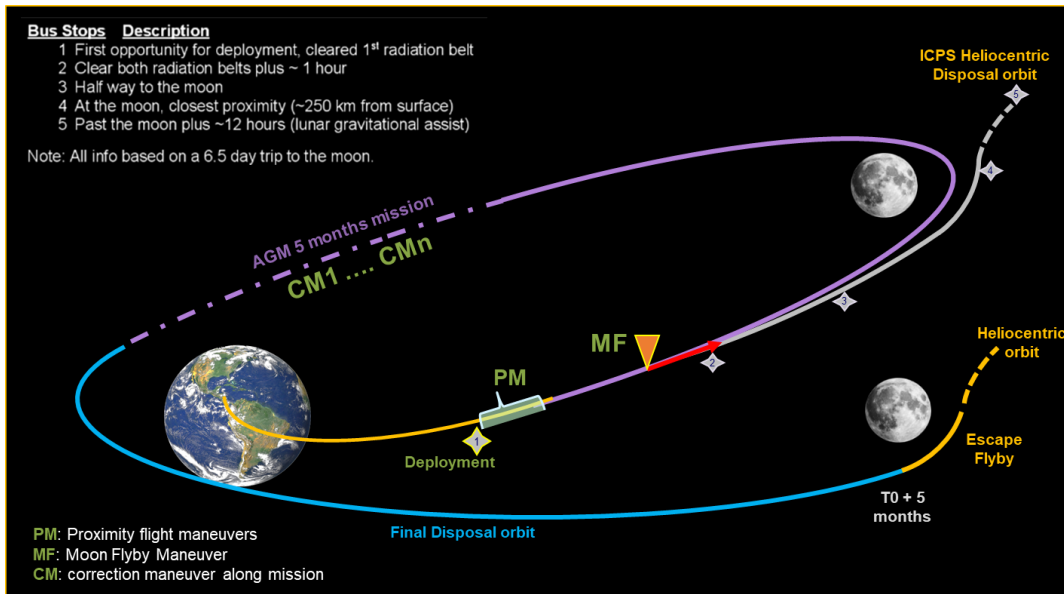


Figure 2-4 ArgoMoon Mission Phases

The last part of the mission, as well as the entire mission itself, is an opportunity to test ArgoMoon technology in a hostile environment: the so-called Deep Space.

2.2 The CubeSat Concept

CubeSat's world is continuously growing as it integrates easily accessible technologies. The priority of these satellites is to bring terrestrial technologies in LEO, minimizing the costs. ArgoMoon satellite identifies itself with the concept of CubeSat, but at the same it integrates deep space equipment that are able to withstand an hostile environment. The spacecraft's dimensions are limited, about 200 mm x 300 mm x 100 mm, in the jargon it is a 6U (someone likes referring to ArgoMoon as a "shoe box"). For this reason the subsystems location must be studied and evaluated to optimize many fundamental aspects such as heat dissipation or the interconnection among elements. Figure 2-5 reports a model of the ArgoMoon spacecraft.

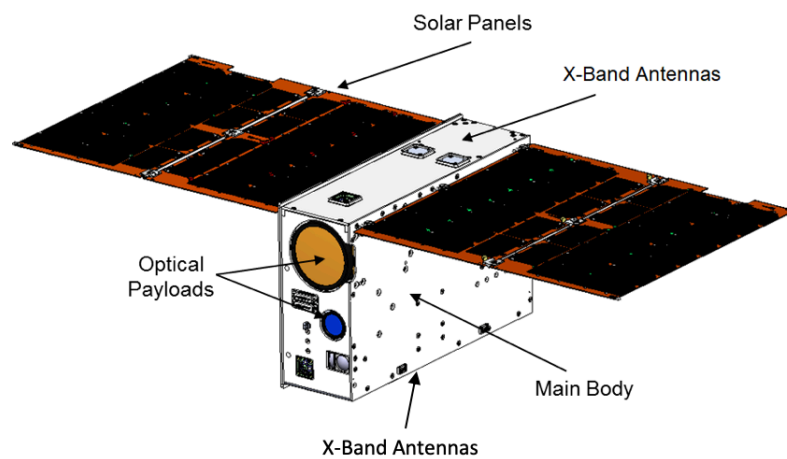


Figure 2-5 ArgoMoon Representation

The lack of space did not allow the installation of deployable antennas. This justifies the choice of fixed patch antennas strategically located. Their positioning has been studied to allow communication with Earth in almost all the phases of the mission and the operative modes of the satellite. Two pairs of X-band antennas (TX/RX) are placed onto opposite sides of the satellite structure to enlarge ground stations visibility.

Chapter 3

Communication System

This chapter provides an overview of the communication system on which ArgoMoon is part. First a quick look at NASA Deep-Space Network with some details on the functionalities and a small introduction to ArgoMoon telecom subsystem. Then, an introduction to telemetry and telecommand services with a summary of all the parameters useful for a link design. At the end, a description of the two ranging systems commonly adopted.

3.1 NASA Deep-Space Network

To communicate with ground, ArgoMoon makes use of one of the most important telecommunication infrastructures on Earth. NASA Deep-Space Network (DNS) is the landmark for interplanetary missions since several years. DSN provides stations array distributed over the Earth surface, strategically located, to assure full spacecraft visibility 24h per day. Figure 3-1 shows how the antennas are located. They are approximately 120 degrees apart in longitude each other.



Figure 3-1 NASA DSN Antenna Location [3]

3.1.1 Ground Station Specifications

In each antenna location, different types of antennas have been installed with different size and characteristics. Nowadays, they make available 70m (for considerable astronomic distances) or 34m antennas. 34m antennas are classified according to two typologies: Beam Waveguide (BWG) and High Efficiency (HEF).

BWG antennas perfectly suit ArgoMoon requirements in terms of operative frequencies and receiver performances. Each antenna has at least one Low Noise Amplifier (LNA) for each supported frequency band and, for the same band, it can support simultaneous Right Circular Polarization (RCP) and Left Circular Polarization (LCP). When simultaneous uplink and downlink of the same polarization are required, reception must be through the diplexer, and the noise will be increased over that of the non-diplexed path. Additionally, all BWG antennas offer a low-gain mode (-20 dB) for use at high received signal power levels for spacecraft near the Earth [4].

In [4] there are all the useful antenna parameters and detailed specifications at different weather conditions and antenna elevation angle to be used for mission planning and link budget analysis.

3.1.2 Frequency Bands Allocation

Given that, ArgoMoon mission is classified as Near-Earth (NE) mission, ArgoMoon spacecraft has to communicate in the frequency bands allocated for this mission typology. NE classification is established according to the maximum reached distance by the satellite. In general, for distances less than 2 million km the mission is classified as NE (or Category A), on the contrary it is classified as Deep-Space (DS) (or Category B). Based on this mission classification, different frequency bands have been allocated by the International Telecommunication Union (ITU). The ones that are supported by DSN are listed in Table 3-1. Some of them are Not Available (NA).

Table 3-1 Frequency Bands (in MHz) Available at DSN Stations

	Near-Earth		Deep-Space	
	Uplink	Downlink	Uplink	Downlink
S-Band	2025-2110	2200-2290	2110-2120	2290-2300
X-Band	7190-7235	8450-8500	7145-7190	8400-8450
K-Band	NA	25500-27000	NA	NA
Ka-Band	NA	NA	34200-34700	31800-32300

Even if not yet supported everywhere, the trend is to move toward higher frequencies (K and Ka band), since at those frequencies there is more available band allowing higher data rates. However, growing in frequency means facing an higher signal attenuation with a subsequent lower Signal-to-Noise Ratio (SNR) at the receiver side.

A spacecraft relatively close to Earth, or on its early mission phase, has a signal strength at the receiving end that is too high with respect to the one received by a satellite from DS. Given that ground receivers work with an insignificant SNR, the stronger signal from a satellite close to Earth acts as interference onto the weaker signal received from DS. This is why there are two different frequency bands for NE and DS. Furthermore, a series of rules have been established at international level to preserve the fragile DS communications.

For the entire ArgoMoon mission, it has been chosen to communicate in X-Band. In particular, following the NE classification, ArgoMoon operative frequency will be within 7190-7235MHz for uplink (from Earth to Spacecraft) and 8450-8500MHz for downlink (from spacecraft to Earth). For convenience, in the rest of the dissertation, the X-Band center frequency will be taken as reference for analysis and results.

3.1.3 DSN Services

DSN stations support telecommand and telemetry services, doppler measurements and range estimation in one-way, two-way or three-way mode. In this sense they provide coherent tracking in case the transponder generates a downlink carrier frequency equal to the uplink carrier frequency multiplied by a rational number, the transponding ratio. Usual transponding ratios are reported in Table 3-2.

Table 3-2 Transponding Ratios

Uplink	Downlink	Ratio (Downlink/Uplink)
S	S	240/221
S	X	880/221
X	S	240/749
X	X	880/749

Other transponding ratio may be employed, but they need to be negotiated through the JPL Frequency Manager.

The customer can buy different services with various characteristics and costs. For instance, in a standard communication scenario a single station might be enough, but in case of more advanced options required by the customer (like Δ -Dor [23]), more than one operative station at time may be employed. Another aspects that can vary the cost are the communication window time duration or how rapid data are going to be delivered to the user after processing. Before every mission, DSN provides the possibility to perform a suite of tests. The main purpose of these test is to establish compatibility between the spacecraft's radio frequency subsystem and DSN stations, as a means to eliminate post launch anomalies and subsequent troubleshooting [8]. Chapter 6 contains a set of tests performed by ArgoMoon spacecraft at DSN's facility DTF-21, in Monrovia (CA).

3.2 ArgoMoon Telecom Subsystem

ArgoMoon telecom subsystem has been designed to guarantee full compatibility with DSN infrastructure. It is in charge of handling all the uplink and downlink functionalities for telemetry, tracking, telecommand and science data. The hardware of ArgoMoon telecom subsystem includes:

- X-Band transponder managing both downlink and uplink communications;
- Low-Noise Amplifier (LNA)
- 4 Watts Solid-State Power Amplifier
- Two TX/RX antenna pairs
- Coaxial cables
- Power and control cables

The transponder is controlled and monitored by the satellite On-Board Computer (OBC).

ArgoMoon spacecraft uses two different antennas for receiving a transmitting signals toward the ground. This way, a full-duplex link is possible without inserting any type of diplexer in the transmission and reception lines.

Figure 3-2 shows an high level block diagram for the ArgoMoon Telecom Subsystem.

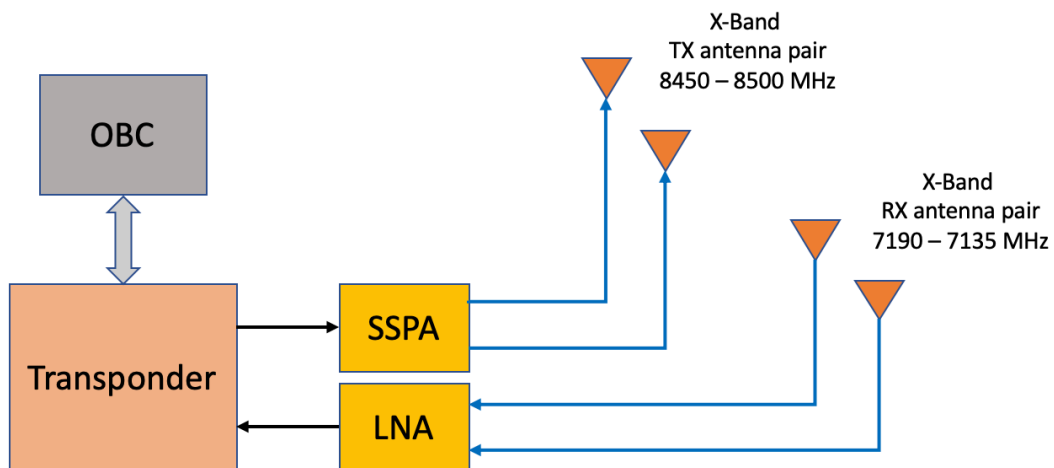


Figure 3-2 ArgoMoon Telecom Subsystem Block Diagram

3.3 Telemetry and Telecommand

The fundamental functions of a satellite require a considerable stable communication to control and command the spacecraft and send useful information toward the Earth. Telemetry (TM) and Telecommand (TC) are the name used to distinguish the data services in the two directions of the satellite link communication. TM refers to the data sent from the satellite to the ground stations, on the contrary, TC refers to the data sent from the ground stations toward the satellite.

3.3.1 Telemetry Overview

A TM system has the purpose to transparently transfer data from a remote space location to an end point located in space or on Earth. Specifically, from this document perspective TM messages are sent from ArgoMoon spacecraft to DNS ground stations. TM data flows consists of house-keeping data, Science or payload data and TC reception status. Figure 3-3 reports the TM system in terms of a layered service model provided by the Consultative Committee for Space Data System (CCSDS¹). It should be noted that, this document only deals with the last two layers of the model by analysing the physical channel link communication, link budget results for all the mission phases, doppler compensations and coding error corrections requirements in order to properly receive TM data.

In order to evaluate the TM system performance, a compatibility test campaign was performed at JPL Development Test Facility (DTF-21) and a set of important results has been reported in Chapter 6.

¹ CCSDS is continuously developing standards for data and information systems. The scope of CCSDS is to enhance cooperation among space agencies and increase multi-agency spaceflight collaboration.

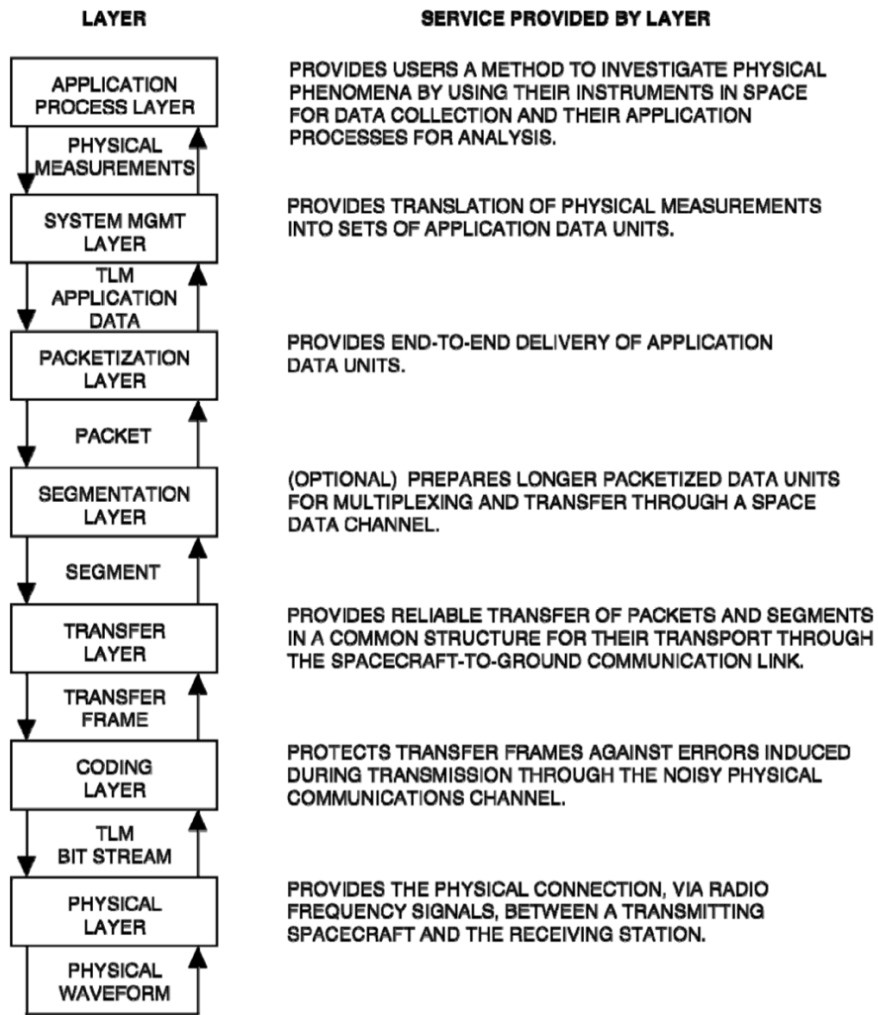


Figure 3-3 Layered Telemetry Service Model [7]

3.3.2 Telemetry: Physical Layer

Content removed due to company confidential information: if interested, please contact Argotec srl.

3.3.3 Telemetry: Systems Loss Models

Content removed due to company confidential information: if interested, please contact Argotec srl.

3.3.4 Telemetry: Coding Layer

The purpose of the telemetry coding layer is to protect user telemetry data against errors caused by a noisy channel. Within the error detecting and correcting capability of the channel code, errors can be detected and corrected at receiver side. Errors occur in a situation in which the energy of the signal is too weak, inducing the receiver to make wrong decision. Typically, in a space channel, this condition happens due to the signal degradation along the propagation path length and the thermal noise in the receiving system (see paragraph 4.3).

Channel coding performance is expressed in term of Bit Error Rate (BER) as function of E_b/N_0 . Performance comparison of different selected codes are shown in Figure 3-4. These performance data are obtained by software simulation, assuming that there are no synchronization losses (like the ones described in the previous paragraph) and the input is constrained to be chosen from between two levels, because BPSK modulation is assumed [7]. In the plot, the lower bound is given by the Shannon's limit performance for a binary input Additive White Gaussian Noise (AWGN) channel and a code rate² $\frac{1}{2}$.

² the code rate R (or information rate) of a forward error correction code is the proportion of the data-stream that is useful (information bits).

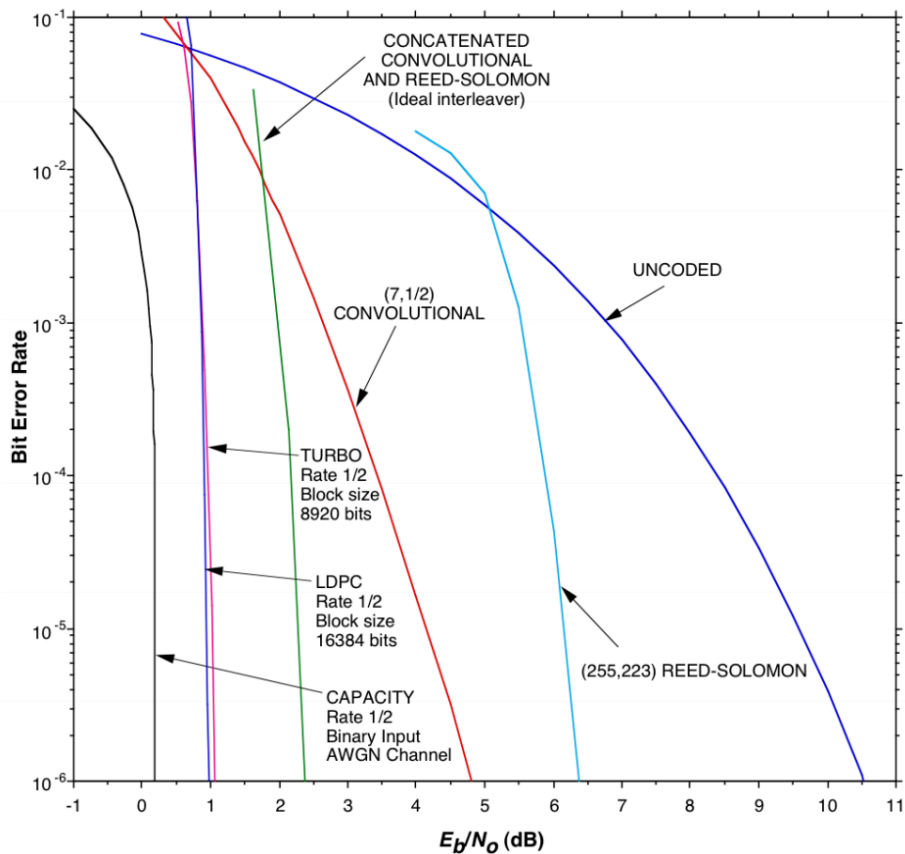


Figure 3-4 Performance Comparison of Selected Convolutional, Reed-Solomon, Concatenated and Turbo Code [7]

It is clear that, Turbo codes can provide very high coding gains. Turbo code performance is within 1 dB the ultimate Shannon limit for codes with rate $\frac{1}{2}$. Low Density Parity Check (LDPC) code, reaches similar performance but doubling the block size. Usually, a very long block size can increase the receiver acquisition time (the time the receiver needs to acquire symbol lock) since it requires a certain number of correct received frame.

In general, increasing the number of redundant bits, or equivaled decreasing the code rate, enhances the code performance. The price is the higher bandwidth occupation due to the higher symbol rate. Figure 3-5 shows the bit rate and symbol rate terminology in a transmission chain.

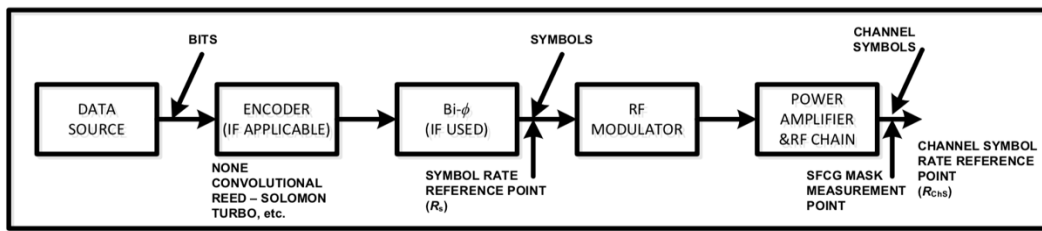


Figure 3-5 Bit Rate and Symbol Rate Terminology [10]

Clearly, to keep the bit rate of the data source constant, the symbol rate must be R times faster (where R is the reciprocal of the code rate) than the bit rate, widening the occupied frequency band. A good compromise for the ArgoMoon mission is the Turbo $\frac{1}{2}$ with block length 8920 bits, or equivalent Turbo(8920, $\frac{1}{2}$). The telemetry data structure for a Turbo code is shown in Figure 3-6.

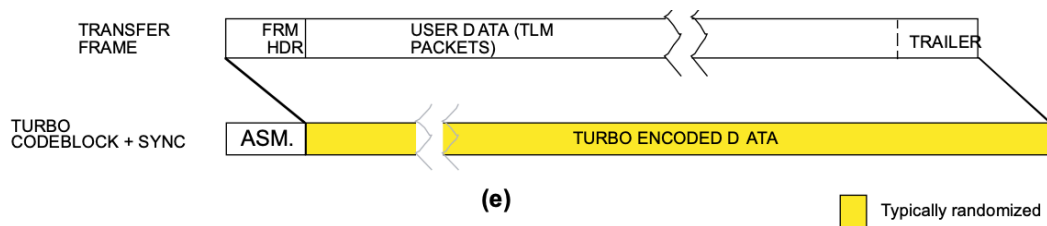


Figure 3-6 Telemetry Data Structure for Turbo Code [7]

To improve bit transitions density, transmitted bits are typically randomized. In case of Turbo coding, the randomization is applied to Turbo codeblock after encoding. By CCSDS standard, the pseudo-random sequence is generated using the following polynomial

$$p(x) = x^8 + x^7 + x^5 + x^3 + 1 \quad (3.1)$$

The generator sequence is initialized with all ones. The length of the sequence is 255. For synchronization purpose, an Attached Sync Marker (ASM) is concatenated in order to let the receiver locate where the randomized Turbo codeblock starts and derandomize it.

3.3.5 Telecommand Overview

A TC system has the purpose to transparently transfer data from Earth to an end point located in space. From this document perspective TC messages are sent from DNS ground stations to ArgoMoon spacecraft. TC data flows consist of direct commands to the spacecraft or application-related commands. The TC system performance has been tested during a compatibility test campaign at JPL DTF-21 and a set of interesting results are reported in Chapter 6.

Figure 3-7 reports the CCSDS TC system structure in terms of sending and receiving end procedures.

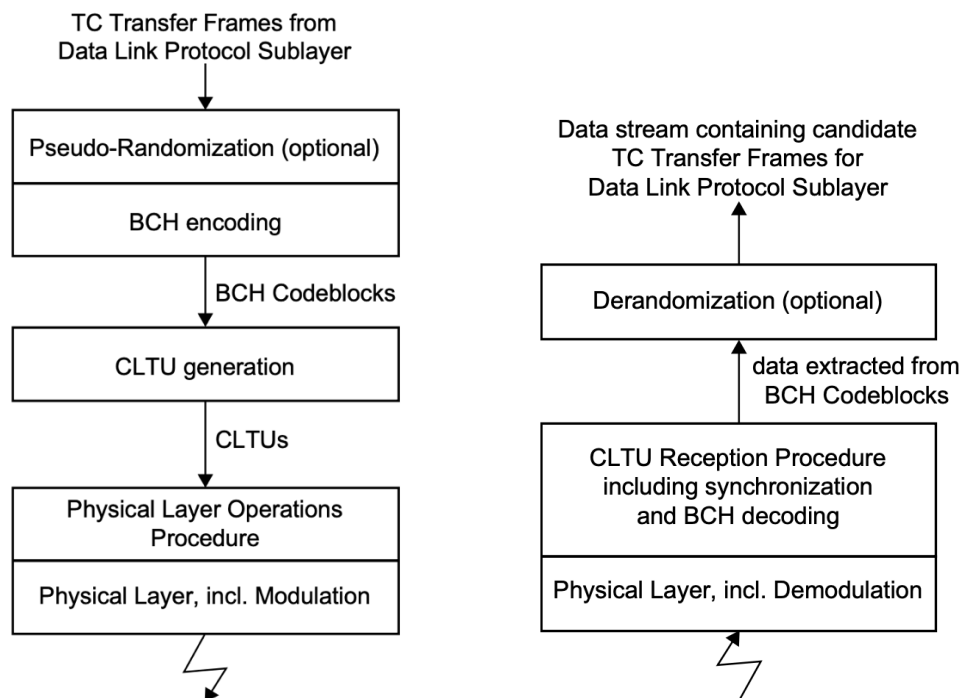


Figure 3-7 Procedures at Sending End (Left) and Receiving End (Right) [21]

Pseudo-randomization is considered optional, and in ArgoMoon mission is not applied, for this reason is will not be discussed in the following paragraphs.

The baseband signal is a Pulse code Modulated (PCM) waveform that is BPSK modulation onto a 16kHz sine-wave subcarrier. This modulation is phase-shift keyed with a signalling level of $\pm 90^\circ$ and resulting in a fully suppressed subcarrier.

[22]

3.3.6 Telecommand: BCH Encoding

Data from upper layer, packed in TC transfer frames, are optionally randomized and then partitioned in blocks of 56 bits to apply a forward error correction coding scheme. The recommended coding scheme by CCSDS standard in [21] is a Bose-Chaudhuri-Hoquenghem (BCH) coding. As for any coding technique, BCH encoding provide protection against errors. Figure 3-8 shows the format of a BCH codeblock.

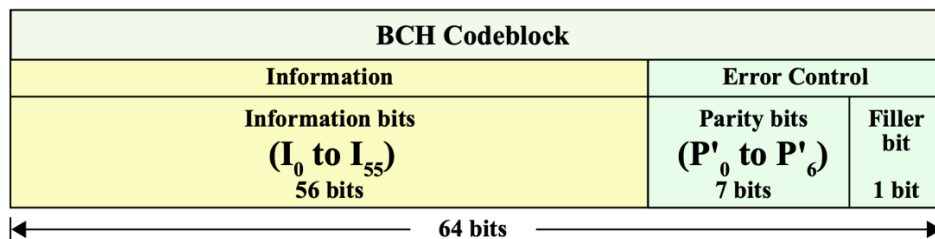


Figure 3-8 Format of a BCH Codeblock [21]

The recommended basic coding scheme uses a basic $(63,57)^3$ Hamming code with a minimum Hamming distance of three bits. This code can either correct a single error or detect two errors, but not both simultaneously. The last bit of the codeblock is just a filler bit and it is always set to zero. The code implementation can be done by means of a linear feedback shift register with generator polynomial

$$g(x) = x^6 + x + 1 \quad (3.2)$$

“In single error correction mode, the decoding of a BCH Codeblock is considered successful if no errors are found or if a single error is found and corrected. If the decoding process detects uncorrectable errors, then the codeblock is rejected.” [21].

³ The code has 6 check bits out of 63 bits of the codeword length. The remaining 57 bits are information bits.

3.3.7 Telecommand: Communication Link Transmission Unit

When BCH codeblocks are generated they are packed in a single structure called Communication Link Transmission Unit, or shortly CLTU. Each CLTU includes fixed start (16 bits) and tail (64 bits) sequences (Figure 3-9) which are considered as CLTU boundaries.

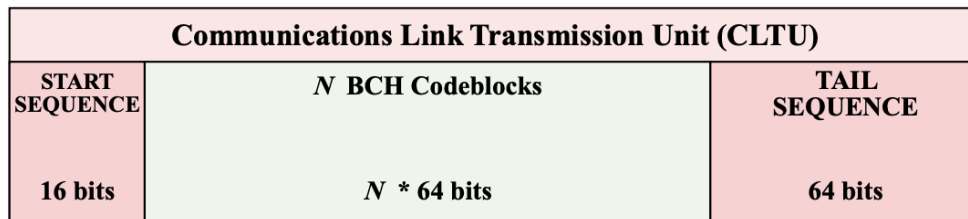


Figure 3-9 Format of a CLTU [21]

Performance for a TC system based on this coding scheme are detailed by CCSDS Green Book in [21], where a careful description has been presented, considering all the possible positions of the wrong bits. Summarizing, most likely errors occur in the portion of a CLTU where the BCH codeblocks are contained since this is the longer part of a CLTU, and the probability of having an error increases. If this is the case, when a BCH codeblock rejection (due to uncorrectable errors) is raised, all the remaining BCH codeblocks will be discarded and the receiver will search a new CLTU looking for the next start sequence. If errors occur in the start sequence, the receiver may ignore that CLTU waiting for a valid start sequence. In case of errors in the tail sequence, there is a risk of erroneously accepting it as valid or correctable BCH codeblock. In this case, the receiver loses the tail sequence and it could miss the next CLTU.

3.3.8 Telecommand: Physical Layer and Operation Procedures

The standard provides two Physical Layer and Operation Procedures (PLOP) named PLOP-1 and PLOP-2.

With PLOP-1, the physical channel is deactivated and reactivated between each CLTU. The bit synchronization is lost for sure, it will be reacquired during the

acquisition sequence⁴ transmitted before each CLTU. The channel throughput is reduced but PLOP-1 can improve reliability avoiding fails in detecting the boundary between CLTUs. With PLOP-2, the physical channel is not deactivated after each CLTU, and an idle sequence ensures that the bit synchronization is maintained. This can provide higher throughput but also troubles in missing start or tail sequences.

Figure 3-10 shows the rejection probability, with PLOP-2 and single error correction mode, for an entire frame coming from upper layer partitioned in a certain number of BCH codeblocks.

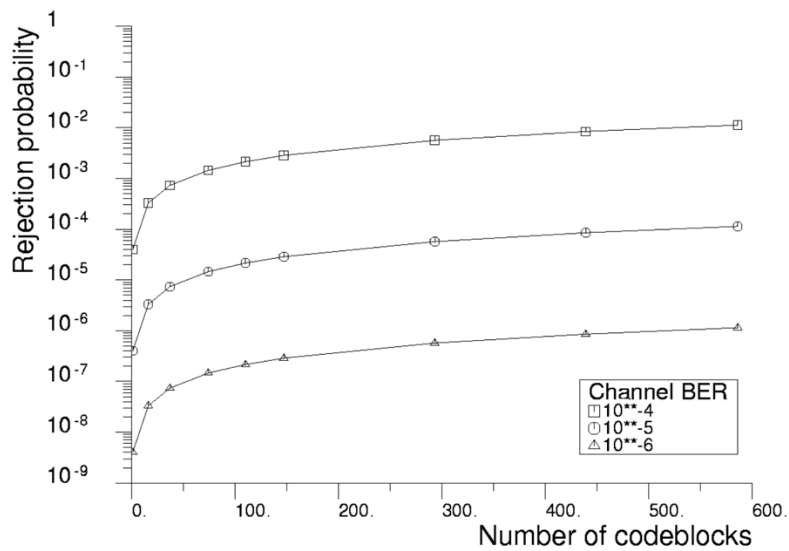


Figure 3-10 Frame Rejection Probability in Single Error Correction Mode for the Last or Only Frame in a CLTU (PLOP-2) [21]

With PLOP-2, if the channel BER is below 10^{-6} , the frame rejection probability is considered small enough, even with large frame size (high number of BCH codeblocks in a CLTU). Due to large ground antennas, high transmitted power and relatively low orbit, for ArgoMoon mission the channel BER is small enough to assure good reliability with PLOP-2 standard.

In the following paragraphs, where the link performances are determined, the channel BER has been derived using the standard formula for an AWGN channel

⁴ The acquisition sequence consists of alternating '1' and '0' bits enabling the receiving end to acquire bit synchronization.

$$BER = \frac{1}{2} \operatorname{erfc} \left(\sqrt{\frac{E_b}{N_0}} \right) \quad (3.3)$$

For results of the TC system performance, see paragraph 5.5.

3.4 Ranging

One of the most important signal components is a signal sent by ground stations used to improve the trajectory model of spacecrafts tracked by the DSN. DSN ranging system provides two kinds of ranging signals based on different principles:

- Sequential Ranging: a range clock signal and other continuous wave (CW) components to solve phase ambiguity [22];
- Pseudo-Noise (PN) Ranging: a logical combination of a range clock and several PN codes [11].

The ground station transmits an uplink carrier that has been phase modulated by the ranging signal. The modulated uplink carrier is received and demodulated by the spacecraft transponder and the recovered ranging signal then phase-modulates the downlink carrier. The DSN receiver demodulates the downlink carrier and measures the round-trip delay experienced by the ranging signal. This technique is coherent because the transponder uses a phase-locked procedure to ensure that the uplink and downlink carriers are coherently related [12]. The fact that, a coherent downlink signal is needed, springs from the lack of synchronization between spacecraft and ground clocks, which directly translates into a measured delay error. This technique, called two-way measurement, overcome the clock synchronization issue. One-way delay measurements are employed in a technique called Differential One-Way Ranging (DOR), which is beyond the scope of this discussion. The last ranging technique is the so-called three-way ranging, used when the round-trip delay is so large that the receiving

station is different from the transmitting one. This way, the delay measure is similar but less accurate than the two-way ranging.

At the customer, the ranging measure ends up being delivered as a phase value expressed in “unit of phase” called Range Unit (RU). The user translates a two-way phase delay (RU) into a two-way time delay using the equation (3.4).

$$Two_way\ time\ delay = \frac{749}{221} * \frac{2 * RU}{f_x} \quad (3.4)$$

where f_x is the uplink carrier frequency.

3.4.1 Sequential Ranging

Content removed due to company confidential information: if interested, please contact Argotec srl.

3.4.2 PN Ranging

Content removed due to company confidential information: if interested, please contact Argotec srl.

Chapter 4

Link Budget Analysis

This chapter provides all the techniques and strategies adopted in the link budget analysis for ArgoMoon mission. Signal attenuation and atmospheric losses are analysed in general. Receiver noise temperatures are differentiated for DSN and ArgoMoon receiver.

4.1 Free Space Path and Atmospheric Losses

Content removed due to company confidential information: if interested, please contact Argotec srl.

4.2 Antenna Gains

The so-called Isotropic Radiator is a theoretical reference antenna used to define the meaning of antenna gain for any other kind of antenna. An isotropic radiator is able to radiate the same amount of power in every directions (for this reason it does not exist but it is only a theoretical model). The term “antenna gain” defines how much power is concentrated from that antenna in a particular direction compared with the power radiated in the same direction by the isotropic radiator, provided that the same power is supplied to both antennas. In Figure 4-1 there is a typical radiation pattern of an antenna. There are a main lobe, which indicates the direction of maximum gain and other side lobes. The antenna gain is quantified by measuring the distance between the diagram and the origin.

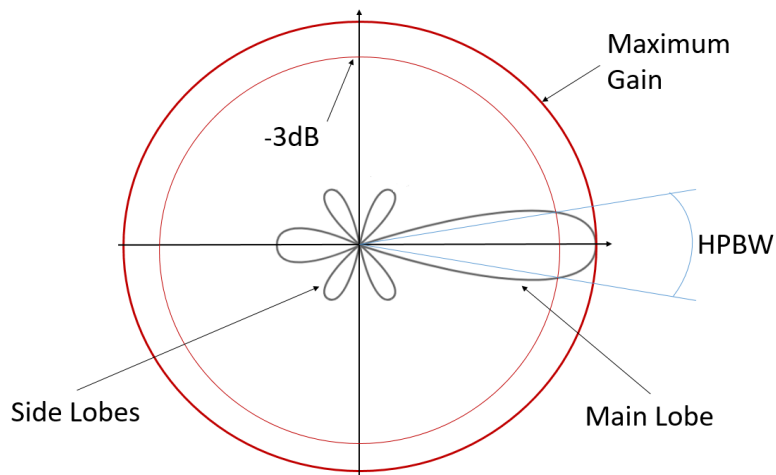


Figure 4-1 Typical Antenna Radiation Pattern

An important parameter is the Half-Power Beam Width (HPBW), expressed in degrees or radians. HPBW represents the angular separation, in which the magnitude of the radiation pattern decreases by 50% (or -3dB) from the peak of the main lobe. In other words, it is the area where most of the power is radiated.

4.2.1 ArgoMoon Antenna Gain

ArgoMoon spacecraft uses two different antennae for receiving and transmitting signals toward the ground. In this way a full-duplex link is possible without any diplexer in the transmission/reception lines. Both TX and RX antennas are small patch antenna with simulated radiation pattern shown in Figure 4-2 for the TX antenna and in Figure 4-3 for the RX antenna. They have a maximum gain close to 7.3dBi and a HPBW approximately equal to 80 degrees.

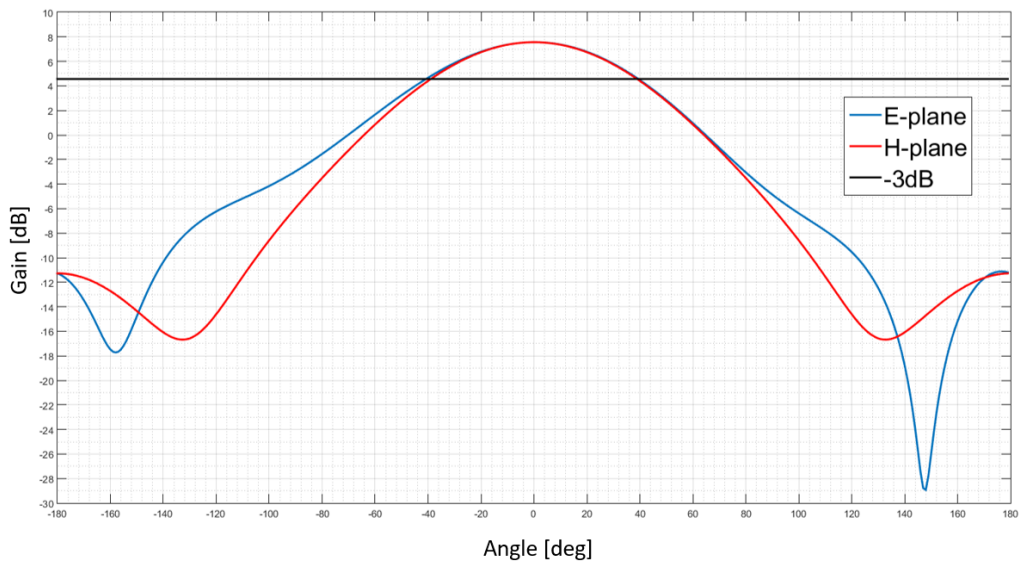


Figure 4-2 Radiation Pattern for TX Antenna (Central Frequency 8.475 GHz)

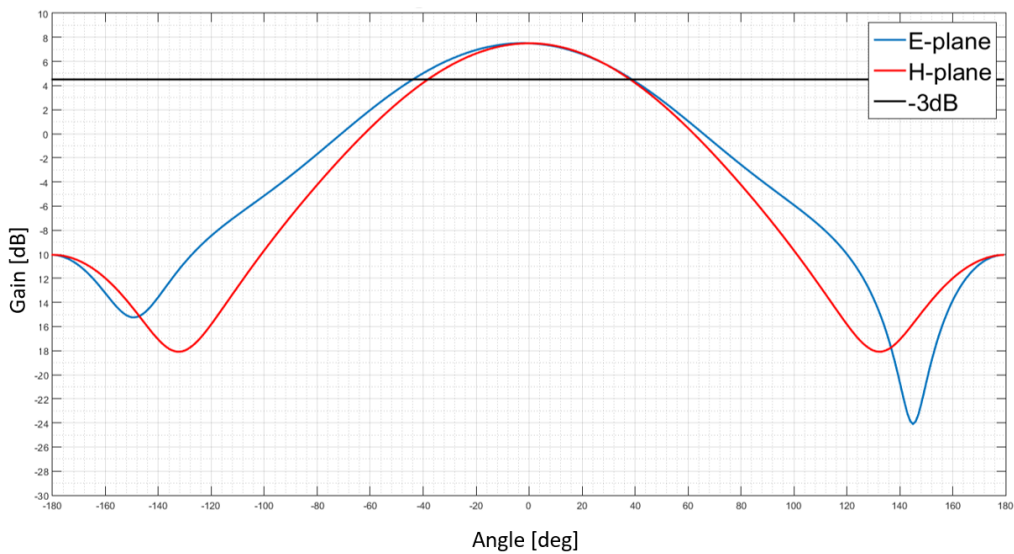


Figure 4-3 Radiation Pattern for RX Antenna (Central Frequency 7.213 GHz)

In this analysis, it is assumed that both antennas have a constant gain of 7.3dBi. Then, a margin of 3dB is imposed to account for pointing error gain reduction of both ground and spacecraft antennas.

4.2.2 DSN Antenna Gain

Large ground antenna offers the possibility to receive very weak signals. The gain of that antennas are huge (a 34-meter antenna reaches 66.98 dBi in nominal conditions), but small variation have to be taken into account in designing a link budget. One reason of gain reduction is due to small structural deformation of materials when the antenna operates at different elevation angles. The model for that phenomenon is provided by the following equation

$$G(\theta) = G_0 - G_1(\theta - \gamma)^2 \text{ [dBi]} \quad (4.1)$$

where

- θ = elevation angle ($6 \leq \theta \leq 90$) [deg]
- G_0 = nominal antenna gain [dBi]
- G_1 [dB] and γ [deg] are station dependent parameter

Furthermore, a deviation from the nominal gain is generated when the antenna operates at a frequency different from the nominal one. The equation that describes this effect is the following

$$G = G_0 + 20\log(f/f_0) \quad (4.2)$$

where

- G_0 = nominal antenna gain [dB]
- f_0 = nominal antenna operative frequency [Hz]
- f = actual antenna operative frequency [Hz]

For operations at higher frequencies in the same band, the antenna gain is increased, on the contrary it is reduced.

An important variation of the antenna gain is the contribution generated by pointing error. The high antenna directivity (or equivalent the narrow main lobe beamwidth) causes a large antenna gain reduction if the pointing accuracy is poor. A margin in the link budget accounts for this gain reduction.

4.3 System Noise Temperatures

The communication link performance is critically dependent on the receiving system noise temperature. Link performances are usually expressed in terms of received signal power-to-noise power spectral density (P/N_0). This ratio is generally evaluated at the input of the receiver by knowing the received signal power and the system operative noise temperature (T_{op}). A simplified model that illustrates the meaning of T_{op} is shown in Figure 4-4.

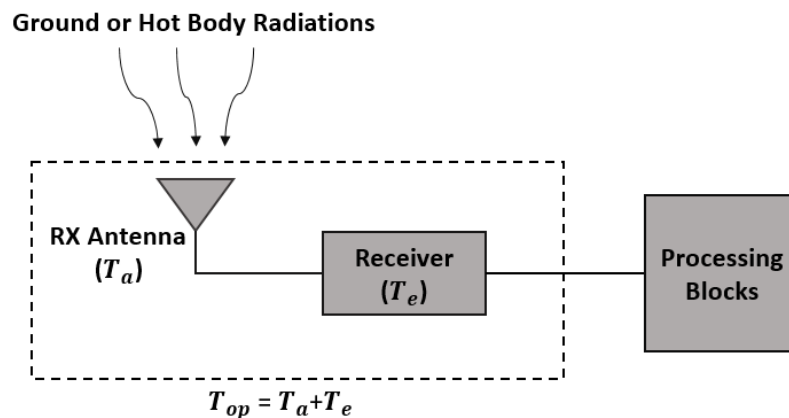


Figure 4-4 Operative Temperature Illustration

T_{op} is the sum between the antenna temperature T_a and the equivalent noise temperature T_e of the receiver.

T_a includes all the interferences captured by the antenna such as electromagnetic radiations coming from hot bodies (any object whose temperature is above the absolute zero radiates electromagnetic energy) or Earth and man-made interferences. The noise power radiated by an object depends not only on its physical temperature but also on the ability of its surface to let the heat leak out. This radiated heat power is associated with the so-called brightness temperature. The brightness temperature is not the same as the physical temperature of the body, but the two temperatures are proportional. In this discussion, the hot body contributions are attributed to a quiet Sun, Moon and Earth and are reported in Table 4-1.

Table 4-1 Hot Body Brightness Temperature at X-Band

Body	Brightness Temperature [K]
Quiet Sun	15000
Moon	250
Earth	300

Man-made interferences are neglected due to high unpredictability and very unluckily to happen in space. However, ground antennas assure high directivity and no interferences should come from the ground. Moreover, international regulations aim at minimizing the inter-interference between different transmissions in space.

Regarding T_e , it includes thermal noise, RF mixer and Intermediate Frequency (IF) contributions, cable losses and everything else that reduces the signal-to-noise ratio. It is usually derived from the receiver noise figure F (it includes most of the contributions) and adding the SNR reduction due to cable losses. In this sense, the noise figure of a cable is exactly equal to the cable loss in dB at the operative frequency.

Once T_a and T_e are known, the noise spectral density N_0 , is computed with the product between the Boltzmann's constant K and the system operative temperature.

$$N_0 = K T_{op} \quad (4.3)$$

Boltzmann constant $K = 1.38064852 \times 10^{-23} \left[\frac{J}{K} \right]$

4.3.1 Noise Temperature for ArgoMoon Receiver

Content removed due to company confidential information: if interested, please contact Argotec srl.

4.3.2 Noise Temperature for DSN Stations

DSN stations are known to be very low-noise receiving systems. A low noise temperature for a satellite system is a strong requirement due to the weak signal received. For a DSN receiver, the sources of noise can be separated into external and internal noise.

Sources of external noise include Cosmic Microwave Background (CMB), Cosmic Microwave Foreground (CMF), galactic and radio sources, solar, lunar and planetary sources, atmospheric (includes lightning), atmospheric absorption, man-made noise and unwanted antenna pick-up. The CMB and the atmosphere are the dominant external noise sources for DNS receiving systems [13].

Sources of internal noise include thermal, shot, current and Barkhausen noise [13]. Thermal noise has a very small contribution thanks to LNAs with paltry noise figure (range from 1.01 to 1.014 which correspond to 3-4 kelvin noise temperature increment).

The system operating noise temperature (T_{op}) for a DNS receiver arises from multiple contributions defined at the feedhorn aperture

$$T_{op} = T_{sky} + T_{ant} + T_{feed} + T_{LNA} + T_f \quad (4.4)$$

where

- T_{sky} = atmospheric and CMB noise
- T_{ant} = antenna noise temperature
- T_{feed} = microwave feed components noise temperature
- T_{LNA} = LNA noise temperature
- T_f = follow-up amplifier noise temperature

All components are expressed in kelvin and they are grouped in two categories:

- T_{sky} accounts for the sky contribution including the atmospheric noise temperature (T_{atm}) and the noise contribution generated by the CMB (T_{CMB}) attenuated along the propagation in the atmosphere
- the so-called antenna microwave system effective noise temperature, T_{AMW} , which includes all the other terms

Now, for convenience, the system operative temperature can be expressed as

$$T_{op} = T_{sky} + T_{AMW} \quad (4.5)$$

DSN Telecommunication Link Design Handbook [15] provides all the tools to compute the temperature contributions stated in the equation above. The model for the computation of the noise temperature is based on the cumulative distribution of weather effects described in the previous paragraph.

Sky contribution is the overall effect of the atmospheric and CMB noise

$$T_{sky} = T_{atm} + T_{CMB} \quad (4.6)$$

The atmospheric noise term is based on the mean effective radiating temperature (T_M) (the temperature of a black body that would emit the same total amount of electromagnetic radiation) and it is modelled to be a function of the cumulative distribution of weather effect

$$T_M = 255 + 25 CD \quad (4.7)$$

where CD is the cumulative distribution of weather effect (weather condition associated in **Error! Reference source not found.**). Then, the final atmospheric contribution is obtained as

$$T_{atm}(\theta) = T_M \left[1 - \frac{1}{L(\theta)} \right] \quad (4.8)$$

where $L(\theta)$ is the atmospheric loss derived in paragraph 4.1, expressed in linear scale. Finally, at DSN receiver the effective CMB temperature is decreased by a factor that depend on the atmospheric attenuation $L(\theta)$.

$$T'_{CMB}(\theta) = \frac{T_{CMB}}{L(\theta)} \quad (4.9)$$

Regarding the antenna microwave component, it can be easily evaluated with the following expression

$$T_{AMW} = T_1 + T_2 e^{-\alpha\theta} \quad (4.10)$$

T_1 , T_2 and α coefficients are provided for each antenna of the three locations into the telecommunications interface modules [4]. θ is the elevation angle expressed

in degree. Table 4-2 report an example of these parameter for one station for each antenna location.

Table 4-2 Antenna Parameters for T_{AMW} Computation

	T_1 [K]	T_2 [K]	α
Goldstone DSS 24	30,39	2,9	0,11
Canberra DSS 34	16,71	5	0,15
Madrid DSS 54	18,31	11	0,15

Finally, the overall system operative temperature is obtained by adding all the noise temperature contributions described above

$$T_{op} = T_{atm}(\theta) + T'_{CMB}(\theta) + T_1 + T_2 e^{-\alpha\theta} \quad (4.11)$$

It is obvious to understand that the final operative temperature only depends on the antenna elevation angle and it takes as parameter the cumulative distribution to account for different weather conditions. The atmospheric models generated for a particular complex should be used for all antennas at that complex, regardless of the small altitude differences among the antennas. Figure 4-5 and Figure 4-6 show the values obtained for the system operative temperature for all the admissible elevation angle ($6 \leq \theta \leq 90$) for two antennas located in two different complexes (Canberra and Goldstone).

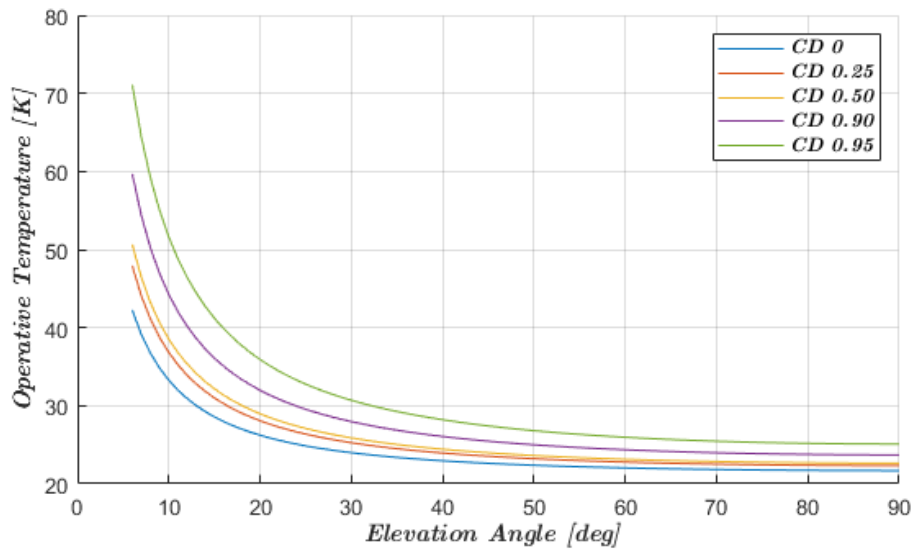


Figure 4-5 Canberra DSS-34 (HEMT Diplexed) System Operative Temperature as Function of Elevation Angle (February)

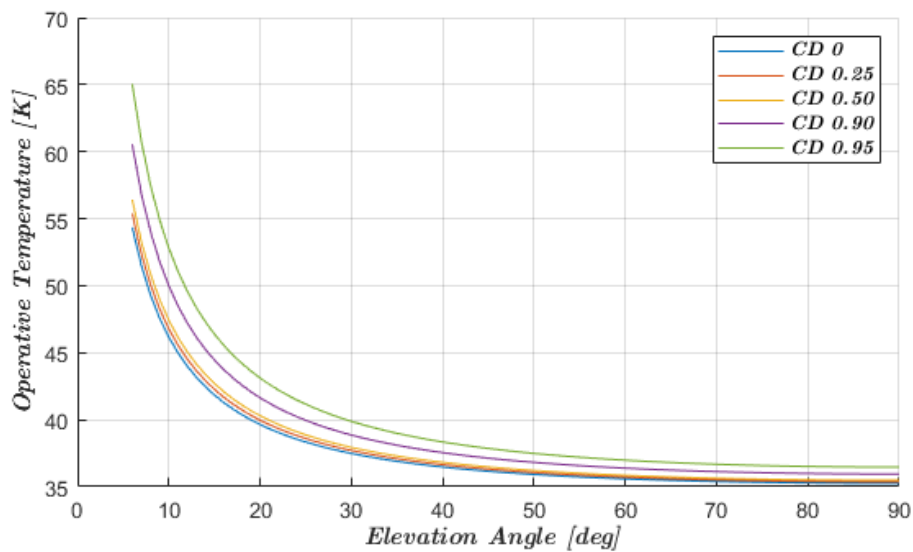


Figure 4-6 Goldstone DSS-24 (Maser Diplexed) System Operative Temperature as Function of Elevation Angle (February)

The last important contribution to the noise temperature for DSN ground station is the so called planetary noise coming from radiated heat power. Since there is no need to track a spacecraft orbiting a planet, and thanks to the tight antenna beam aperture, influence from Moon, Sun or other planetary contribution is neglected. ArgoMoon will be eclipsed beyond the Moon, but in this situation there

will be no communication with ground. Moreover, a smart way to choose communication windows should assure no presence of sun or other planets beyond the spacecraft.

Chapter 5

Mission Analysis and System Performances

This chapter provides information extracted from ArgoMoon mission analysis, including ground station parameters and system performances evaluation in two communication scenarios.

5.1 ArgoMoon Mission Phase 1

ArgoMoon mission starts with the attempt of the satellite to contact the ground. The first communication window is the most important one. It has the main task to send fundamental information to the OBC for synchronization and coordination purposes (time synchronization will be lost during the months spent inside the launcher).

After the release from ICPS, ArgoMoon will be approximately at 31000km of altitude from Earth. From mission analysis tools and orbit estimation, very likely the first visible ground station will be located in Madrid. This ground station will be able to see ArgoMoon with a favorable elevation angle allowing a reliable communication.

Table 5-1 through Table 5-3 report some of the physical parameter for each antenna complex during Phase 1. Some of them are omitted in case the spacecraft is Not Visible (NV) from the station. These parameter are the starting point in the system performance evaluation. The first column reports the time reference for the respective parameter in the same row. The second column reports the ArgoMoon (AGM) absolute altitude with respect of Earth center of mass. The third column lists the satellite elevation angles as seen by that particular antenna complex. From that elevation angle and using equation **Error! Reference source n**

ot found. the relative distance is reported in the next column. Then, the relative velocity, which is an important parameter that will be used during satellite acquisition to predict the uplink carrier, applying doppler compensation. The last three columns provide relatives angles which are:

- the angle between ArgoMoon and the Sun from an observer on Earth, and considering the Sun far enough, it is the angle between the Earth-ArgoMoon joining line and the Sun as seen by ArgoMoon (see Figure 5-1);
- the angle between ArgoMoon and the Moon from an observer on Earth. In case the satellite is eclipsed beyond the Moon, this angle is close to zero.
- the angle between Earth and Moon as seen by ArgoMoon (see Figure 5-1).

Table 5-1 Phase 1 - Goldstone Ground Station Fundamental Estimated Parameters

GOLDSTONE							
GREG DATE [dd-mm-yy hh:mm:ss]	AGM altitude [km]	Elev Ang [deg]	Distance [km]	Relative Velocity [km/s]	AGM- Sun Angle [deg]	AGM- Moon Angle [deg]	Earth- Moon Angle [deg]
27-Jun-20 21:08:03	NV	NV	NV	NV	NV	NV	NV
27-Jun-20 22:38:38	NV	NV	NV	NV	NV	NV	NV
27-Jun-20 23:42:51	63905	8.25	62678	2.76	131	56	122
28-Jun-20 01:38:03	83223	25.45	80278	2.38	135	55	121
28-Jun-20 02:14:43	88835	30.30	85441	2.32	135	55	120
28-Jun-20 03:48:05	102254	39.13	98101	2.22	137	54	119
28-Jun-20 06:23:23	122399	35.99	118534	2.18	138	49	113
28-Jun-20 07:23:23	129597	29.01	126376	2.18	138	49	112

Table 5-2 Phase 1 - Canberra Ground Station Fundamental Estimated Parameters

CANBERRA							
GREG DATE [dd-mm-yy hh:mm:ss]	AGM altitude [km]	Elev Ang [deg]	Distance [km]	Relative Velocity [km/s]	AGM- Sun Angle [deg]	AGM- Moon Angle [deg]	Earth- Moon Angle [deg]
27-Jun-2021:08:03	NV	NV	NV	NV	NV	NV	NV
27-Jun-20 22:38:38	NV	NV	NV	NV	NV	NV	NV
27-Jun-20 23:42:51	NV	NV	NV	NV	NV	NV	NV
28-Jun-20 01:38:03	NV	NV	NV	NV	NV	NV	NV
28-Jun-20 02:14:43	NV	NV	NV	NV	NV	NV	NV
28-Jun-20 03:48:05	NV	NV	NV	NV	NV	NV	NV
28-Jun-20 06:23:23	122399	17.33	120354	1.69	140	51	111
28-Jun-20 07:23:23	129597	29.49	126341	1.64	140	51	110

Table 5-3 Phase 1 - Madrid Ground Station Fundamental Estimated Parameters

MADRID							
GREG DATE [dd-mm-yy hh:mm:ss]	AGM altitude [km]	Elev Ang [deg]	Distance [km]	Relative Velocity [km/s]	AGM- Sun Angle [deg]	AGM- Moon Angle [deg]	Earth- Moon Angle [deg]
27-Jun-20 21:08:03	31210	38.79	26810	4.37	93	38	132
27-Jun-20 22:38:38	51623	30.87	48053	3.56	120	39	131
27-Jun-20 23:42:51	63905	23.17	61120	3.24	125	40	129
28-Jun-20 01:38:03	83223	6.22	82289	2.90	129	43	126
28-Jun-20 02:14:43	88835	0.25	88579	2.82	131	44	125
28-Jun-20 03:48:05	NV	NV	NV	NV	NV	NV	NV
28-Jun-20 06:23:23	NV	NV	NV	NV	NV	NV	NV
28-Jun-20 07:23:23	NV	NV	NV	NV	NV	NV	NV

Based on information contained in the three previous tables, two stations are enough to cover the whole ArgoMoon Phase 1. These stations are located in Madrid (MDRID) for the first part of Phase 1 then in Goldstone (GLDST) for the remaining communication window. Summarizing, useful link parameters are provided in Table 5-4.

Table 5-4 Phase 1 - Ground Station and Link Parameters

GREG DATE [dd-mm-yy hh:mm:ss]	Ground Station	Distance [km]	Uplink Doppler [Hz]	Atm. Attenuation [dB]	Downlink FSPL [dB]	Uplink FSPL [dB]
27-Jun-20 21:08:03	MDRID	26810.45	105140.5	0.170784	199.58	198.18
27-Jun-20 22:38:38	MDRID	48052.70	85488.97	0.208529	204.64	203.24
27-Jun-20 23:42:51	MDRID	61120.09	78121.12	0.271918	206.73	205.33
28-Jun-20 01:38:03	GLDST	80277.74	57272.09	0.134959	209.10	207.70
28-Jun-20 02:14:43	GLDST	85440.55	55713.55	0.114974	209.64	208.24
28-Jun-20 03:48:05	GLDST	98100.89	53398.88	0.091909	210.84	209.44
28-Jun-20 06:23:23	GLDST	118533.79	52424.36	0.098698	212.49	211.09
28-Jun-20 07:23:23	GLDST	126375.88	52318.05	0.119580	213.04	211.64

The first new piece of information is the doppler frequency (carrier frequency shift seen by ArgoMoon) derived from the uplink carrier frequency and the relative velocity between the ground station and the spacecraft. Then, there are the atmospheric attenuation and the FSPL, computed as described in paragraph 4.1. The atmospheric attenuation has been evaluated taking a cumulative distribution of 0.99 (the worst possible condition). As normal, weather monthly statistics are more adverse in Madrid with respect to Goldstone, in which the weather is expected to be more sunny and drier on June. So that, the atmospheric attenuation is higher in general for Madrid’s antenna complex.

Uplink signal power can be tuned by DSN transmitters to maintain the spacecraft received power within recommended limits (to cause no damage). The suggested minimum transmitted power is 23dB, which is the value that will be considered for this performance analysis. From the provided elevation angle, DSN effective TX and RX gains are computed as described in paragraph 4.2.2. The same for the DSN receiver operative temperature, computed as reported in paragraph 4.3.2 and listed in Table 5-5. Considering FSPL, atmospheric attenuation, DSN gains and ArgoMoon antenna gain (see paragraph 4.2.1), by means of Friis formula in equation **Error! Reference source not found.**, the uplink and downlink received signal powers are provided in Table 5-5.

Table 5-5 Phase 1 - Receivers Parameters

Greg. Date [dd-mm-yy hh:mm:ss]	Elevation Angle [deg]	DSN Effective RX Gain [dB]	DSN Effective TX Gain [dB]	DSN RX Power [dB]	AGM RX Power [dB]	DSN Top [K]
27-Jun-20 21:08:03	39	67.90	66.76	-121.74	-104.29	31.75
27-Jun-20 22:38:38	31	67.88	66.74	-126.87	-109.41	34.13
27-Jun-20 23:42:51	23	67.85	66.71	-129.06	-111.60	38.19
28-Jun-20 01:38:03	25	67.87	66.72	-131.27	-113.81	41.77
28-Jun-20 02:14:43	20	67.88	66.74	-131.78	-114.32	40.46
28-Jun-20 03:48:05	39	67.90	66.76	-132.93	-115.48	38.96
28-Jun-20 06:23:23	35	67.89	66.75	-134.59	-117.13	39.40
28-Jun-20 07:23:23	29	67.88	66.73	-135.18	-117.73	40.76

ArgoMoon operative temperature has been computed by analysing the communication scenario for Phase 1. Figure 5-1 shows how ArgoMoon receiver will be placed in space with respect to Earth, Moon and Sun as soon as it will be deployed by ICPS. To avoid over-complicating the dissertation, it is assumed that the spacecraft is able to point toward the ground stations without any pointing error. To account for a finite pointing accuracy a margin of 3dB is taken in the final result. In general, ArgoMoon will perform manoeuvres to maintain an attitude that permits to take advantage of the solar rays, catching power from the solar panels. Then, It will use the most appropriate antenna pair.

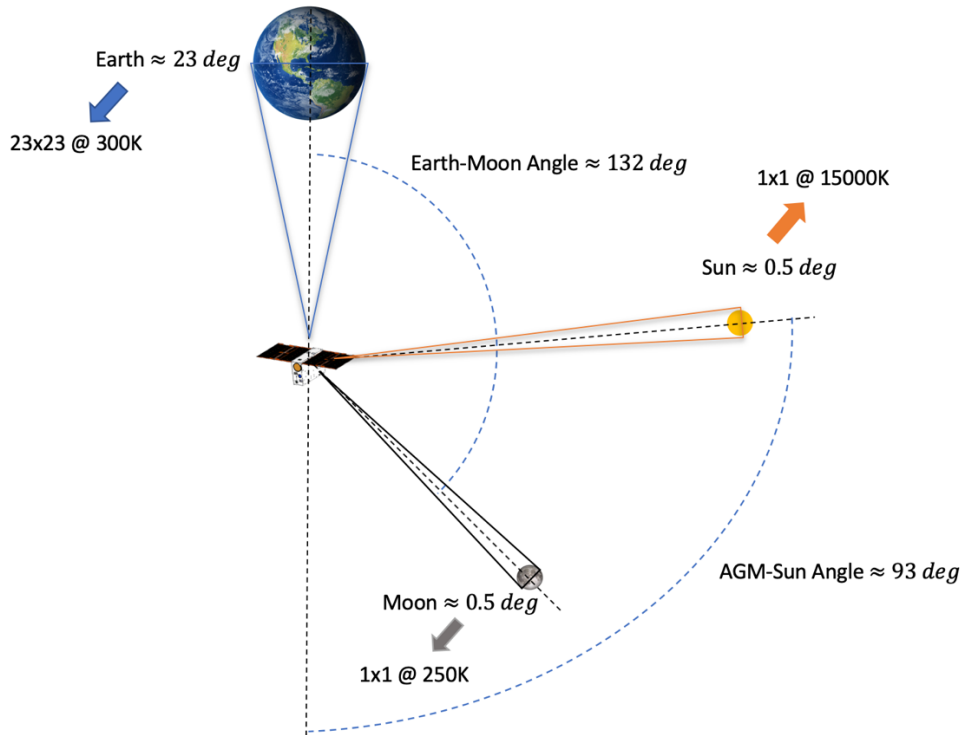


Figure 5-1 Phase 1 - First Acquisition Communication Scenario - ArgoMoon Altitude 31210 km

Assuming an altitude from Earth of approximately 31000km, Figure 5-1 shows how wide are Earth, Moon and Sun for ArgoMoon antennas. Paragraph 4.3.1 provides a method to compute the antenna noise temperature using an approximated approach. In this situation, Earth, Moon and Sun temperature contributions have been approximated by a square matrix of size $N \times N$, with N equal to the rounded aperture of the body seen by the satellite in degrees. The antenna temperature is equal to **9.43K**. This value is for a worst case scenario: Earth accounts for most of the antenna temperature and, at the minimum altitude (after ArgoMoon deployment), it will be maximum. ArgoMoon's antenna temperature is assumed constant for the entire Phase 1.

5.2 ArgoMoon Mission Phase 2

Due to the impossibility to reports all the result for the entire Phase 2, only one significant situation is going to be discussed: few moments after the last lunar fly-by. The relevance of this scenario comes from the high satellite altitude and

the stronger influence by the Moon due to its nearness. As reported in Table 5-6, from Canberra (CNBRR), it is possible to track the spacecraft just after the eclipse beyond the Moon. In this situation, the ground station sees the spacecraft with a very small angle from the Moon (penultimate column) and, from now on, the satellite will speed up and will enter an heliocentric orbit.

Table 5-6 Phase 2 - Canberra Ground Station Fundamental Estimated Parameters

CANBERRA							
GREG DATE [dd-mm-yy hh:mm:ss]	AGM altitude [km]	Elev Ang [deg]	Distance [km]	Relative Velocity [km/s]	AGM- Sun Angle [deg]	AGM- Moon Angle [deg]	Earth- Moon Angle [deg]
10-Dec-20 19:23:23	414558	38.99	410520	0.71	55	3	18
10-Dec-20 20:23:23	417241	49.14	412402	0.78	55	3	18
10-Dec-20 21:23:23	420196	56.83	414849	0.86	55	3	17
10-Dec-20 22:23:23	423459	59.98	417931	0.95	55	3	17
10-Dec-20 23:23:23	427044	57.23	421673	1.04	54	3	17
11-Dec-20 00:23:23	430941	49.80	426054	1.12	54	3	16
11-Dec-20 01:23:23	435118	39.82	431011	1.19	54	3	16

As for Phase 1, link parameters such as doppler frequency, FSPL and atmospheric attenuation are reported in Table 5-7. The atmospheric attenuation has been evaluated taking a cumulative distribution equal to 0.99.

Table 5-7 Phase 2 - Ground Station and Link Parameters

GREG DATE [dd-mm-yy hh:mm:ss]	Ground Station	Distance [km]	Uplink Doppler [Hz]	Atm. Attenuation [dB]	Downlink FSPL [dB]	Uplink FSPL [dB]
10-Dec-20 19:23:23	CNBRR	410520	17126	0.25587	223.23	221.83
10-Dec-20 20:23:23	CNBRR	412402	18776	0.21286	223.28	221.88
10-Dec-20 21:23:23	CNBRR	414849	20736	0.19234	223.35	221.95
10-Dec-20 22:23:23	CNBRR	417931	22864	0.18595	223.42	222.01
10-Dec-20 23:23:23	CNBRR	421673	25005	0.19148	223.49	222.09
11-Dec-20 00:23:23	CNBRR	426054	27008	0.21078	223.57	222.17
11-Dec-20 01:23:23	CNBRR	431011	28729	0.25144	223.65	222.25

DSN receiver noise temperature and uplink and downlink received powers are reported in Table 5-8. It is interesting to notice how DSN operative temperature

increase at smaller elevation angles due to the stronger influence by Earth's atmosphere.

Table 5-8 Phase 2 - Receivers Parameters

Greg. Date [dd-mm-yy hh:mm:ss]	Elevation Angle [deg]	DSN Effective RX Gain [dB]	DSN Effective TX Gain [dB]	DSN RX Power [dB]	AGM RX Power [dB]	DSN Top [K]
10-Dec-20 19:23:23	38.99	67.9017	66.7576	-145.48	-128.03	34.87
10-Dec-20 20:23:23	49.14	67.9025	66.7584	-145.50	-128.04	32.26
10-Dec-20 21:23:23	56.83	67.886	66.7419	-145.55	-128.10	31.01
10-Dec-20 22:23:23	59.98	67.8749	66.7309	-145.63	-128.17	30.62
10-Dec-20 23:23:23	57.23	67.8847	66.7406	-145.70	-128.24	30.95
11-Dec-20 00:23:23	49.80	67.9016	66.7576	-145.78	-128.32	32.13
11-Dec-20 01:23:23	39.82	67.90	66.76	-145.90	-128.45	34.60

Figure 5-2 shows the communication scenario just after the lunar fly-by. It is worth to notice that, in this situation, ArgoMoon will communicate with the opposite antenna pair to let the solar panel catching power from the Sun.

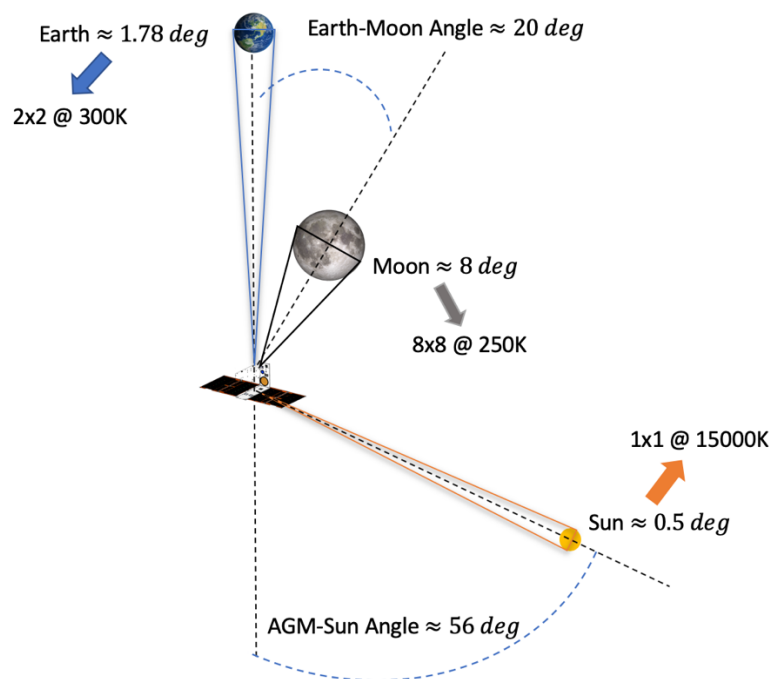


Figure 5-2 Phase 2 – After Last Lunar Fly-by Communication Scenario - ArgoMoon Altitude 409768 km

Following the same consideration made for Phase 1 ArgoMoon antenna temperature is equal to **3.56K**. Here most of the noise contribution comes from the Moon.

5.3 Power Allocation

Content removed due to company confidential information: if interested, please contact Argotec srl.

5.4 Telemetry Performance

Telemetry performances have been evaluated assuming uplink and downlink modulation indexes in **Error! Reference source not found.**

Table 5-9 reports effective modulation indexes and the downlink power allocation based on the equation provided in paragraph 5.3 in case of non-regenerative ranging channel, with a noise equivalent bandwidth of 1.5MHz.

Table 5-9 Phase 1 - Downlink Power Allocation

Greg. Date [dd-mm-yy hh:mm:ss]	θ_r [rad pk]	θ_c [rad pk]	θ_n [rad pk]	Carrier Suppression [dB]	P_D / P_T [dB]	P_R / P_T [dB]
27-Jun-20 21:08:03	0,22243	0.22243	0,00448	-11.9881	-0.5143	-28.0005
27-Jun-20 22:38:38	0,22237	0.22237	0,00838	-11.9878	-0.5139	-28.0025
27-Jun-20 23:42:51	0,22230	0.22230	0,01140	-11.9874	-0.5135	-28.0049
28-Jun-20 01:38:03	0,22217	0.22217	0,01537	-11.9867	-0.5128	-28.0093
28-Jun-20 02:14:43	0,22215	0.22215	0,01603	-11.9865	-0.5127	-28.0101
28-Jun-20 03:48:05	0,22207	0.22207	0,01797	-11.9861	-0.5122	-28.0128
28-Jun-20 06:23:23	0,22189	0.22189	0,02185	-11.9851	-0.5112	-28.0191
28-Jun-20 07:23:23	0,22178	0.22178	0,02379	-11.9845	-0.5106	-28.0227

This is an approximation based on the analysis provided in [24]. Such an approximation is less accurate in case of low noise power (during early mission phase). But in general it works very well in case of higher noise power level.

Once the power allocation has been performed, it is possible to estimate downlink system performances using equations in paragraphs 3.3.2 and 3.3.3. For most of

the ArgoMoon mission, telemetry modulation index is designed to have a residual carrier, which is necessary in case telemetry and ranging are sent simultaneously. Table 5-10 lists the system margins during the whole mission Phase 1. The link margin has been obtained from the effective E_b/N_0 removing 3dB of losses due to pointing accuracy and 1.4dB required by the Turbo decoder to achieve the error floor, that for Turbo(8920, 1/2) is assumed at 6.77×10^{-6} BER.

Table 5-10 Phase 1 - Telemetry Performances and Link Margin @ 256kbps

Greg. Date [dd-mm-yy hh:mm:ss]	Carrier Loop SNR [dB]	η_{Radio}	η_{Sym}	η_{Sys}	Effective E_b/N_0 [dB]	Link Margin [dB]
27-Jun-20 21:08:03	22.067	0.92965	0.99999	0.89499	36.76	32.36
27-Jun-20 22:38:38	22.065	0.92961	0.99998	0.89494	31.32	26.92
27-Jun-20 23:42:51	22.062	0.92957	0.99997	0.89488	28.65	24.25
28-Jun-20 01:38:03	22.057	0.92948	0.99995	0.89479	26.04	21.64
28-Jun-20 02:14:43	22.056	0.92947	0.99995	0.89477	25.68	21.28
28-Jun-20 03:48:05	22.053	0.92942	0.99994	0.89471	24.68	20.28
28-Jun-20 06:23:23	22.045	0.92929	0.99992	0.89458	22.98	18.58
28-Jun-20 07:23:23	22.041	0.92922	0.99991	0.89450	22.24	17.83

The same results are reported for Phase 2 in Table 5-11 and Table 5-12. As expected, the link margin is smaller but still positive to allow correct data decoding.

In both Phase 1 and Phase 2 more than 10dB margin is maintained onto the carrier loop SNR. However, it is worth to notice how the carrier loop SNR reduction is very small from Phase 1 to Phase 2 even with a so large difference in the FSPL. In Phase 1 the high symbol energy has a stronger effect on the carrier loop SNR degradation (equation **Error! Reference source not found.**).

Table 5-11 Phase 2 - Downlink Power Allocation

Greg. Date [dd-mm-yy hh:mm:ss]	θ_r [rad pk]	θ_c [rad pk]	θ_n [rad pk]	Carrier Suppression [dB]	P_D / P_T [dB]	P_R / P_T [dB]
10-Dec-20 19:23:23	0.21545	0.21545	0.07606	-11.9497	-0.47585	-28.243
10-Dec-20 20:23:23	0.21649	0.21649	0.07029	-11.9553	-0.48147	-28.206
10-Dec-20 21:23:23	0.21690	0.21690	0.06784	-11.9576	-0.48373	-28.191
10-Dec-20 22:23:23	0.21704	0.21704	0.06699	-11.9583	-0.48448	-28.187
10-Dec-20 23:23:23	0.21702	0.21702	0.06713	-11.9582	-0.48436	-28.187
11-Dec-20 00:23:23	0.21687	0.21687	0.06800	-11.9574	-0.48358	-28.192
11-Dec-20 01:23:23	0.21656	0.21656	0.06984	-11.9558	-0.48189	-28.203

Table 5-12 Phase 2 - Telemetry Performances and Link Margin @ 256kbps

Greg. Date [dd-mm-yy hh:mm:ss]	Carrier Loop SNR [dB]	η_{Radio}	η_{Sym}	η_{Sys}	Effective E_b/N_0 [dB]	Link Margin [dB]
10-Dec-20 19:23:23	21.83	0.92555	0.99962	0.89071	12,62627	8.22627
10-Dec-20 20:23:23	21.84	0.92584	0.99964	0.891004	12,95032	8.55032
10-Dec-20 21:23:23	21.85	0.92594	0.99964	0.891101	13,06362	8.66362
10-Dec-20 22:23:23	21.85	0.92592	0.99964	0.891085	13,0459	8.64590
10-Dec-20 23:23:23	21.84	0.92582	0.99964	0.890982	12,92839	8.52839
11-Dec-20 00:23:23	21.83	0.92560	0.99962	0.890761	12,68447	8.28447
11-Dec-20 01:23:23	21.80	0.92517	0.99960	0.890325	12,23947	7.83947

5.5 Command Performance

Command performances have been evaluated assuming uplink modulation indexes provided in **Error! Reference source not found.** and power allocation provided in **Error! Reference source not found.**. As stated in paragraph 3.3.8, the minimum required channel BER is 10^{-6} that corresponds to E_b/N_0 equal to 10.53dB (by inverting equation (3.3)). To compute the value of E_b/N_0 perceived by the transponder it is assumed a noise figure equal to 3.5dB (see paragraph 4.3.1) and an antenna noise temperature computed previously. Table 5-13 and Table 5-14 reports performances and system margins for Phase 1 and Phase 2.

The link margin has been obtained considering an extra 3dB of losses due to pointing accuracy and a minimum 10.53dB of E_b/N_0 required.

Table 5-13 Phase 1 - Command Performances and Link Margin @ 4kbps

Greg. Date [dd-mm-yy hh:mm:ss]	AGM Received Power [dB]	Carrier Power [dB]	Command Power [dB]	E_b/N_0 [dB]	Link Margin [dB]
27-Jun-20 21:08:03	-104.29	-104.70	-117.91	49.01	35.48
27-Jun-20 22:38:38	-109.41	-109.82	-123.03	43.88	30.35
27-Jun-20 23:42:51	-111.60	-112.01	-125.22	41.70	28.17
28-Jun-20 01:38:03	-113.82	-114.22	-127.43	39.48	25.95
28-Jun-20 02:14:43	-114.32	-114.73	-127.94	38.98	25.45
28-Jun-20 03:48:05	-115.48	-115.89	-129.10	37.82	24.29
28-Jun-20 06:23:23	-117.13	-117.54	-130.75	36.16	22.63
28-Jun-20 07:23:23	-117.72	-118.14	-131.35	35.57	22.04

Table 5-14 Phase 2 - Command Performances and Link Margin @ 4kbps

Greg. Date [dd-mm-yy hh:mm:ss]	AGM Received Power [dB]	Carrier Power [dB]	Command Power [dB]	E_b/N_0 [dB]	Link Margin [dB]
10-Dec-20 19:23:23	-128.03	-128.43	-141.64	25.34	11.81
10-Dec-20 20:23:23	-128.04	-128.45	-141.66	25.33	11.80
10-Dec-20 21:23:23	-128.10	-128.50	-141.71	25.27	11.74
10-Dec-20 22:23:23	-128.17	-128.58	-141.79	25.20	11.67
10-Dec-20 23:23:23	-128.24	-128.65	-141.86	25.12	11.59
11-Dec-20 00:23:23	-128.32	-128.73	-141.94	25.04	11.51
11-Dec-20 01:23:23	-128.45	-128.85	-142.06	24.92	11.39

5.6 Sequential Ranging Performance

Content removed due to company confidential information: if interested, please contact Argotec srl.

5.7 Pseudo-Noise Ranging Performance

Content removed due to company confidential information: if interested, please contact Argotec srl.

Chapter 6

Compatibility and Functional Tests

This chapter reports test performed directly onto the flight hardware in order to asses DSN compatibility. Then, a description of a Ground Support Equipment for further functional tests to be performed in Argotec (Turin) after the satellite assembly.

6.1 DSN Compatibility Tests

DSN Compatibility test program had the objective to assess ArgoMoon satellite to DSN interface performance and compatibility. These tests have been carried out at DSN's facility DTF-21, in Monrovia (CA).

During the compatibility test, the test setup including ArgoMoon transponder, On-Board Computer and laboratory equipment was inside a screen room (a sort of Faraday cage) in order to mitigate, as much as possible, the effect of possible interferences coming from external environment. The RF connection through a coaxial cable was established with a Compatibility Test Trailer (CTT), outside the DTF-21 building. ArgoMoon team and DSN personnel communicated each other with telephone terminal. Figure 6-1 provides a high-level test configuration block diagram. The following paragraphs summarize all the performed tests.

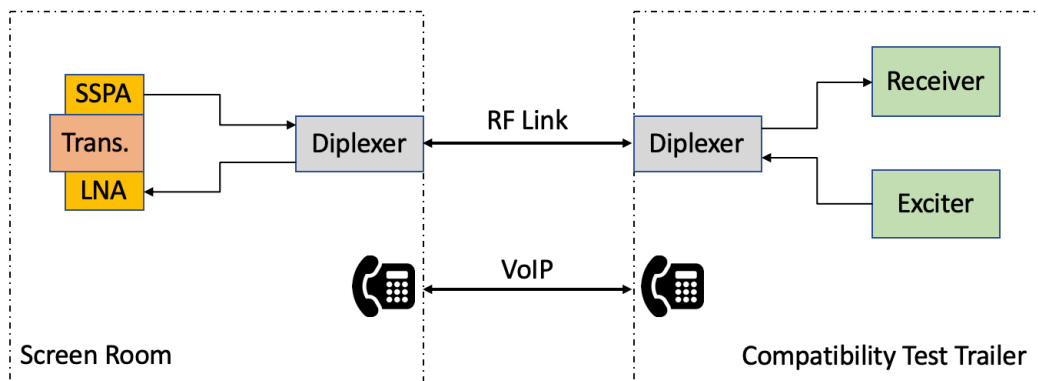


Figure 6-1 Transponder-to-CTT Connection

6.1.1 RF Link Calibration

The purpose of this test was to calibrate the setup for both uplink and downlink transmissions. The outcome of the calibration has been used to characterize the transponder performance that resulted from the subsequent tests.

Variable attenuators (see Figure 6-2) are inserted in the transmission line in order to adjust power level at receiver input in both directions.

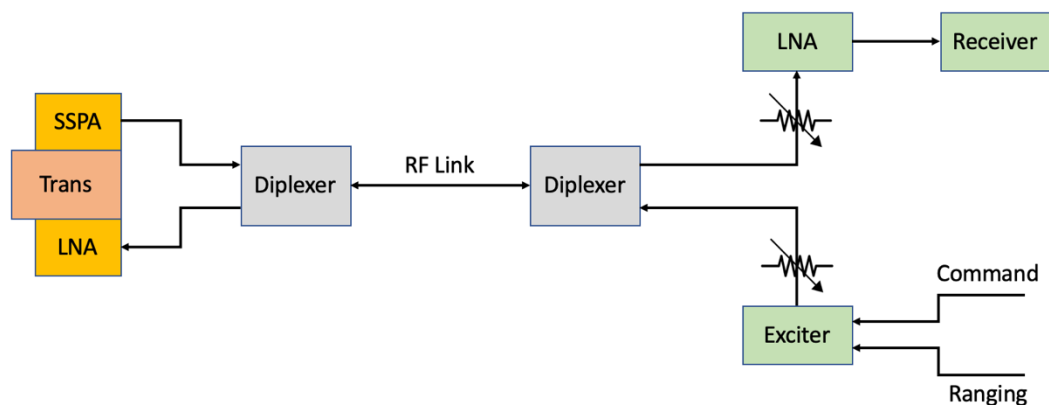


Figure 6-2 Transponder-to-CTT connection. Variable Attenuations

Setting up the attenuator at 0dB attenuation, the power level at transponder LNA input has been measured with a power meter. This power level was assumed to be the hottest signal that could be sent to the transponder. Adding attenuations, it is possible to characterize the behaviour of the transponder at different signal power to noise power spectral density ratio. The same calibration has been

performed on the downlink branch in order to tune the power level at DSN LNA input.

6.1.2 Uplink Receiver Threshold and AGC Calibration

This test aimed at verifying the uplink receiver sensitivity, that is the minimum power level required by the transponder in order to maintain symbols, subcarrier and carrier lock in different transmission conditions.

The test has been performed by increasing the attenuation along the uplink path in order to have a variable power level at transponder LNA input. Starting from the hottest signal and decreasing the power, the AGC values has been recorded.

6.1.3 Uplink Receiver Acquisition and Tracking

This test aimed at verifying the receiver capacity to lock onto a swept carrier and to keep the lock. This test has an important outcome since it follows the strategy to permit the spacecraft transponder to acquire carrier lock. During the satellite acquisition, ground stations perform a sweep in frequency until the carrier lock is acquired by the spacecraft. This is done to compensate the doppler effect which moves the transponder Best Lock Frequency (BLF) away from the nominal value. The sweep profile is shown in Figure 6-3.

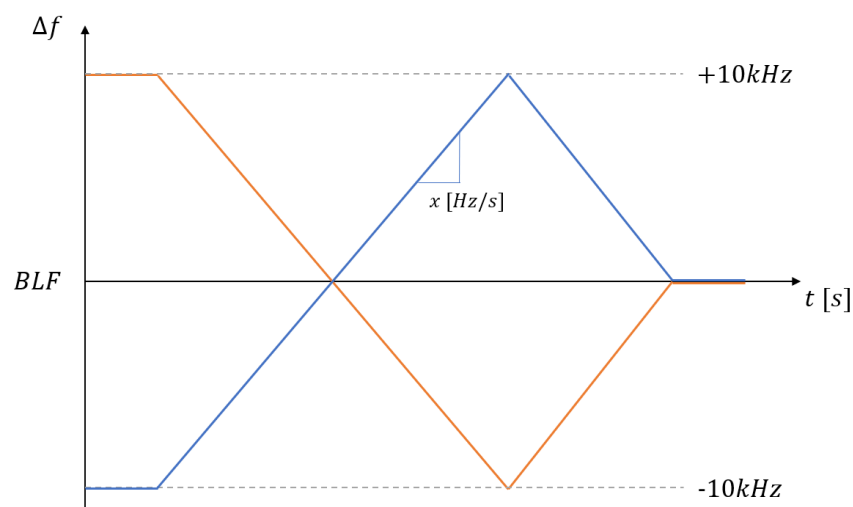


Figure 6-3 Frequency Sweep Profile for Carrier Acquisition and Tracking

The test has been performed in two directions and with a determined sweep rate. The outcome of the test was the minimum amount of power needed at received side per sweep direction to lock onto the carrier.

6.1.4 Uplink Receiver Tracking Range

This test aimed at verifying if the transponder was able to track a swept uplink carrier frequency up to +/- 20 kHz away from the operative frequency (BLF). The test was performed with a constant power level at LNA input and a determined sweep rate in two directions. The sweep profile is shown in Figure 6-4.

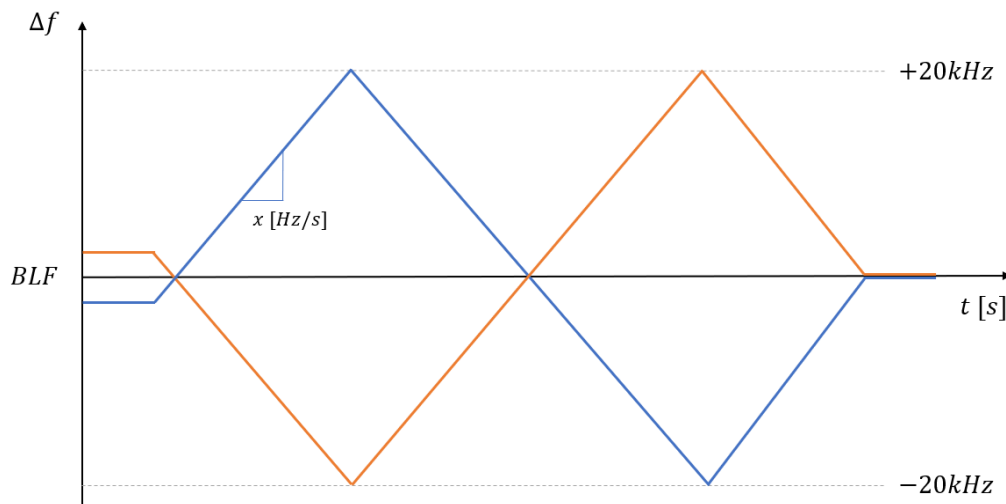


Figure 6-4 Frequency Sweep Profile for Carrier Tracking Range

The pass criteria of the test was the transponder had to be able to maintain the lock for the entire sweep range.

6.1.5 Command and Telemetry Performance

The purpose of this test was to find the minimum amount of power required by receivers to correctly decode command and telemetry.

For command, this test aimed at finding the transponder received power threshold at different data rates, in case of TC-only and TC + Ranging, in order to

be able to correctly receive commands. The test was declared successful every time the transponder was able to receive ten no-operation commands in a CLTU. For telemetry, this test aimed at verifying the power threshold for DSN receiver at different configurations and data rates. The test was declared successful every time the Turbo decoder was able to correct all the errors inside a frame given a certain number of frames to be processed. The minimum number of frames was established by accounting for the transmission time for each data rate.

6.1.6 Range Delay and Polarity

The purpose of this test was to find the delay introduced by the transponder RX/TX chains and its modulation polarity. An initial calibration has been performed by measuring the delay introduced by the entire test setup. Then, for each TX/RX antenna pair the transponder ranging delay has been recorded. The outcome of this test is an essential transponder delay estimation that will be subtracted to the range measurements in order to get the round trip time experienced by the ranging signal during its propagation in space.

6.2 Ground Support Equipment for Functional Tests

Content removed due to company confidential information: if interested, please contact Argotec srl.

Chapter 7

Final Remarks

7.1 Conclusion

This thesis work managed to reach all the objectives discussed in Chapter 1. After an in-depth study on satellite communications, standards and recommendations, the focus has been moved toward the X-Band communication system involved in the mission.

Explore and study all the parts the communication system is composed of

The whole communication system has been studied and its description is provided in Chapter 3. Starting from DSN ground stations, their characteristics and functionalities passing through all the involved standards, uplink and downlink signals composition. Great attention has been given to ArgoMoon telecom subsystem with particular focus onto the transponder even if its dissertation is less rich due to confidential information.

Analyze the satellite link

- **Signal attenuation, atmospheric effects and signal propagation delay**

Two main effects have been studied. First the Free Space Path Loss, derived from the Friis equation which gives the larger contribution. Then the atmospheric attenuation in both water vapor and dry air, which gives a minor attenuation term. In particular, Earth's atmosphere resulted almost transparent for X-Band transmissions. An interesting aspect is the induced delay onto signal propagation that could compromise satellite distance measurements. Results about ranging systems are given in terms of error variance due to noise contribution. Great influence would be given by the

solar corona in case of small angle between the signal propagation direction and the Sun. However, this contribution has been neglected for ArgoMoon ranging system since the spacecraft orbits close to Earth.

- **Receivers and noise contribution**

DSN and ArgoMoon receivers have been studied and terms of their operative noise temperature. Noise term for DSN station is described in DSN Telecommunication Link Design Handbook and it is mostly related to the antenna elevation angle. ArgoMoon receiver noise temperature comes from transponder specifications and antenna noise temperature.

Analyze and evaluate performances

All the information about the communication system and the satellite link have been used to take out a set of system performances. Chapter 5 provides a series of results for different communication scenarios.

Put up mission control tables to allow optimal communication windows allocation during the mission

Mission control table has been built combining information extracted from mission analysis and orbit estimation. These tables contain all the required information for the satellite link and systems margins. An excerpt is included in the description of system performance in Chapter 5 for both uplink and downlink transmission and Phase 1 and Phase 2 of the mission.

Compatibility and functional test of the flight hardware

Compatibility tests have been carried out at DSN facility DTF-21. They proved complete compatibility between ArgoMoon telecom subsystem and DSN's infrastructure. In-depth performances have been measured. The results show that they are all in line with hardware specification. Sometime transponder capabilities were even better than expected. Explicit results have been omitted since they are considered confidential information.

Preliminary functional tests have been performed with a GSE to assess correct uplink and downlink operation involving Argotec's MCC.

7.2 Future Works

At the end of this thesis there are two works which are still on-going.

ArgoMoon in heliocentric orbit

Link performances have been evaluated up to the end of Phase 2. After that, ArgoMoon satellite will enter an heliocentric orbit by changing completely the communication scenario. Higher signal attenuation with subsequent different communication parameters have to be analyzed. Possible Sun contribution to ranging delay and other aspects need to be taken into account.

ArgoMoon functional tests

After the final satellite assembly, a series of functional tests are going to be performed in order to determine proper system functionalities

References

- [1] NASA, *SPIE Secondary Payload Interface Definition & Requirements Document*, March 16, 2015
- [2] Space Launch System, <https://www.nasa.gov/exploration/systems/sls>, October 9, 2018
- [3] Deep Space Network NOW, <https://eyes.nasa.gov/dsn/dsn.html>
- [4] Jet Propulsion Laboratory, *"34-m BWG Stations Telecommunications Interfaces"*, DSN No. 810-005, 104, Rev. J, January 12, 2018
- [5] Jet Propulsion Laboratory, *"Frequency and Channel Assignments"*, DSN No. 810-005, 201, Rev. C, December 15, 2014
- [6] Jet Propulsion Laboratory, *"Doppler Tracking"*, DSN No. 810-005, 202, Rev. C, January 22, 2019
- [7] CCSDS GREEN BOOK, *"TM Synchronization and Channel Coding - Summary of Concept and Rationale"*, CCSDS 130.1-G-2, November 2012
- [8] *"NASA's Mission Operations and Communications Services"*, January 2009
- [9] SFCG, *"Efficient Spectrum Utilisation for Space Research Service (Category A) and Earth Exploration-Satellite Service on Space-to-Earth Links"*, Recommendation SFCG 21-2R4, August 2015
- [10] CCSDS GREEN BOOK, *"Bandwidth-Efficient Modulations - Summary of Definition, Implementation, and Performance"*, CCSDS 413.0-G-3, February 2018
- [11] Jet Propulsion Laboratory, *"Pseudo-Noise and Regenerative Ranging"*, DSN No. 810-005, 214, Rev. A, October 28, 2015
- [12] By Jeff B. Berner, Senior Member IEEE, Scott H. Bryant, and Peter W. Kinman, Senior Member IEEE, *"Range Measurement as Practiced in the Deep Space Network"*, November 2007
- [13] Charles T. Stelzried, Arthur J. Freiley, and Macgregor S. Reid, *"System Noise Concepts with DSN Applications"*, February 2008
- [14] Jet Propulsion Laboratory, *"Atmospheric and Environmental Effects"*, DSN No. 810-005, 105, Rev. E, October 2015

- [15] Jet Propulsion Laboratory, *“DSN Telecommunications Link Design Handbook”*, DSN No. 810-005, February 2019
- [16] Jet Propulsion Laboratory, Joseph H. Yuen, *“Deep Space Telecommunications Systems Engineering”*, July 1982
- [17] Recommendation ITU-R P.676-11, *“Attenuation by atmospheric gases”*, September 2016
- [18] Jet Propulsion Laboratory, *“Telemetry General Information”*, DSN No. 810-005, 206, Rev. C, May 2017
- [19] Jet Propulsion Laboratory, *“34-m and 70-m Telemetry Reception”*, DSN No. 810-005, 207, Rev. A, June 2003
- [20] V. Vilnrotter, A. Gray, and C. Lee, *“Carrier Synchronization for Low Signal-to-Noise Ratio Binary Phase-Shift-Keyed Modulated Signals”*, November 1999
- [21] CCSDS GREEN BOOK, *“TC Synchronization and Channel Coding - Summary of Concept and Rationale”*, CCSDS 230.1-G-2, November 2012
- [22] Jet Propulsion Laboratory, *“Sequential Ranging”*, DSN No. 810-005, 203, Rev. C, October 2019
- [23] Jet Propulsion Laboratory, *“Delta Differential One-way Ranging”*, DSN No. 810-005, 210, Rev. B, February 2017
- [24] Peter W. Kinman, Jeff B. Berner, *“Two-way Ranging During Early Mission Phase”*, 2003